REPUBLIQUE ALGERIENNE DEMOCRATIQUE ET POPULAIRE

MINISTERE DE L'ENSEIGNEMENT SUPERIEUR ET DE LA RECHERCHE SCIENTIFIQUE

Université de Mohamed El-Bachir El-Ibrahimi - Bordj Bou Arreridj

Faculté *des Sciences et de la technologie*

Département d'Electronique

Mémoire

Présenté pour obtenir

LE DIPLOME DE MASTER

FILIERE : ELECTRONIQUE

Spécialité : Industries Electroniques

Par

- **CHOUITER Oussama**
- **HAOUAM Aymen**

Intitulé

Intégration de l'énergie photovoltaïque dans le réseau électrique à l'aide d'un onduleur multi-niveaux de type PUC

Evalué le : ……

Devant le Jury composé de :

Nom & Prénom	*Grade*	*Qualité*	*Etablissement*
M.		*Président*	*Univ-BBA*
M. TALBI Billel	*MCB*	*Encadreur*	*Univ-BBA*
M.	*….*	*Examinateur*	*Univ-BBA*

Année Universitaire 2021/2022

PEOPLE'S DEMOCRATIC REPUBLIC OF ALGERIA

MINISTRY OF HIGHER EDUCATION AND SCIENTIFIC RESEARCH

University of Mohamed El-Bachir El-Ibrahimi - Bordj Bou Arreridj

Faculty of Science and Technology

Department of Electronics

Presented to obtain

THE DIPLOMA OF MASTER

FIELD: Electronics

Speciality: Electronic Industries

By:

- **CHOUITER Oussama**
- **HAOUAM Aymen**

Entitled

Integration of photovoltaic energy into the utility grid using a PUC multi-level inverter

Evaluated on: ….

By the evaluation committee composed of:

Full Name	***Grade***	***Quality***	***Establishment***
M.		***Président***	***Univ-BBA***
M. TALBI Billel	***MCB***	***Encadreur***	***Univ-BBA***
M.	***….***	***Examinateur***	***Univ-BBA***

Academic year 2021/2022

Acknowledgements:

In the name of ALLAH, the Most Gracious and the Most Merciful. Thanks to ALLAH who is the source of all the knowledge in this world, for the strengths and guidance in completing this thesis.

First of all, this work would have not been possible without the help and guidance of Dr. B. TALBI, we thank him for the quality of his exceptional supervision, for his patience, his availability during the preparation of this thesis, his moral support, encouragement, for everything and we really appreciate deeply all what Dr. B. TALBI did for us.

We are aware that we have been honoured by the president of the jury and the examiner for agreeing to review this work. And a special thanks to ABANOU Hocine for uncountable help opportunities also our thanks go to all the teachers, the professors, our parents, our brothers, our sisters, our dear friends, for their help and their sacrifices.

Table of Contents

List of Figures

List of Tables

List of Acronyms and symbols

DPC Direct Power Control

GPV Photovoltaic Generator

IncCon Incremental Conductance

MPPT Maximum Power Point Tracking

P&O Perturb and Observe

AC Alternative current

HB Half-bridge

FB Full-bridge

THD Total harmonic distortion

MLI Multi-level inverter

CHB Cascade h-bridge

NPC Neutral point clamped

FC Flying capacitor

PUC Packed unit cell

MPC Model predictive control

PI Proportional integral

PWM Pulse width modulation

PLL Phase-locked loop

Vdc DC-link voltage

Cdc DC-link capacitor

Ig* Grid reference current

ig Grid current

vg Grid voltage

g Cost function

f Grid frequency

L Rectifier side load inductor

S1, 2,3, Switching signals of the inverter Vs Grid voltage

PI Proportional integral

General Introduction

Nowadays, the world depends heavily on non-renewable energy sources such as coal, oil and natural gas. Meanwhile, energy production is a major challenge in the coming years due to the increasing energy needs, which leads to an increase the environmental pollution caused by previous sources. As a solution for this crisis, the world has begun to use another type of energy called renewable energies, for example, wind energy, solar energy, and biomass. Because it is characterized by unlimited sources and does not affect negatively the environment [1].

Among all renewable energy sources, solar photovoltaic (PV) energy is becoming increasingly competitive with conventional energy sources. Where, the grid-connected PV energy is one of the fastest growing and most promising renewable energy sources in the world [2]. The grid-connected PV systems are broadly classified into two categories, single and two conversion stages. The efficiency resulting from these systems depends not only on the working conditions, but also on the complete conversion chain. This can be achieved by a judicious choice of configurations or topologies, good sizing of components and effective control techniques.

Recently, the application of model predictive control (MPC) in energy conversion systems has been extensively investigated both theoretically and experimentally. Different MPC techniques have been proposed to control multi-level inverters in grid-tied operation, permitting high performance and fast dynamics.

The purpose of this work is to design an effective control scheme based on MPC approach for a single-phase grid-connected photovoltaic system using a PUC (packed U-cell) multi-level inverter. The PUC converter is considered as promising topologies to interface the PV system to grid with less harmonic filters and high efficiency. Unlike other SPMLI topologies, this converter provides 5-level output voltage with only single DC source and six power switches. This work is organized into two chapters:

- The first chapter is dedicated to PV systems, particularly single-phase grid connected PV systems, as well power electronics interfacing topologies for these systems and the control objectives of them.

- In In the second chapter, we will be modelling and controlling a grid-connected PV system based on PUC multi-level using model predictive control technique.

Finally, a general conclusion and perspectives conclude this work.

Chapter I:

Overview of Single-Phase Grid-Connected Photovoltaic Systems

I.1. Introduction

Recently, the penetration of the renewable energy resources into the utility grid has been widely studied by many research projects due to important features of such resources, such as cleanliness and sustainability. Among all renewable energy resources, photovoltaic (PV) energy is increasingly becoming mainstream and competitive with classic sources of energy [3].

This chapter presents an overview on single-phase grid-connected PV systems in order to explain PV energy and illustrate PV systems with their classes. Also, power electronics interfacing topologies for grid connected PV systems and the control objectives of these systems are presented respectively.

I.2. Photovoltaic energy

Photovoltaic energy is a type of renewable, sustainable and non-polluting energy. It is obtained by converting sunlight into electricity using a technology based on the PV effect. This phenomenon was first discovered in 1839 by Edmond Becquerel. When doing experiments

involving wet cells, he noted that the voltage of the cell increased when its silver plates were exposed to the sunlight [4]. The PV effect occurs in solar cells. These solar cells are composed of two different types of semiconductors - a p-type and an n-type - that are joined together to create a p-n junction. By joining these two types of semiconductors, an electric field is formed in the region of the junction as electrons move to the positive p-side and holes move to the negative n-side. This field causes negatively charged particles to move in one direction and positively charged particles in the other direction. Light is composed of photons, which are simply small bundles of electromagnetic radiation or energy. These photons can be absorbed by a PV cell, the type of cell that composes PV panels When light of a suitable wavelength is incident on these cells, energy from the photon is transferred to an atom of the semiconducting material in the p-n junction. Specifically, the energy is transferred to the electrons in the material. This causes the electrons to jump to a higher energy state known as the conduction band, this movement of the electron as a result of added energy creates two charge carriers [4]. A diagram of this process is shown in Figure I.1.

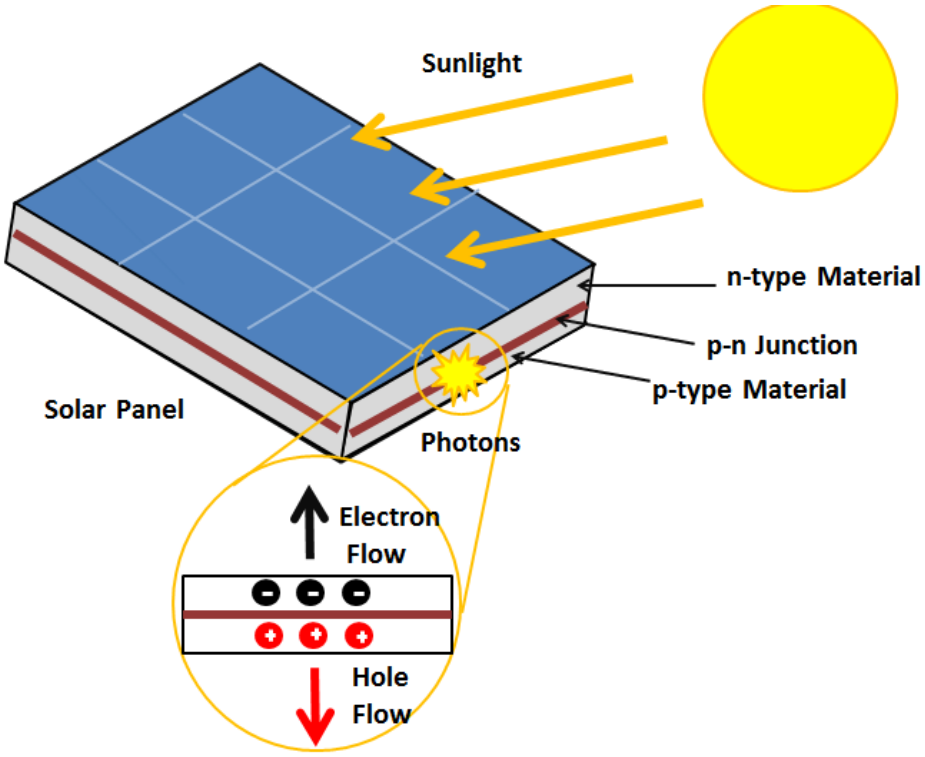

Figure I.1. A diagram showing the photovoltaic effect.

I.3. Photovoltaic system

PV systems are solar energy supply systems, which either supply power directly to an electrical equipment or feed energy into the public electricity grid. PV cells are typically combined into modules that hold up to 72 cells, a number of these modules are mounted in PV

arrays that can measure up to several meters on a side. In general, a PV system consists of PV modules and power electronics converters; PV modules are responsible for converting the sunlight into electricity, then the obtained solar power is processed through the power electronics converters. Usually, a DC-DC converter is employed to regulate the DC power delivered from the PV modules. Then, the DC-DC converter is followed by a DC-AC converter, which process the delivered power from the DC-DC stage and feed it to the AC loads [5]. Figure I.2 shows a typical PV system.

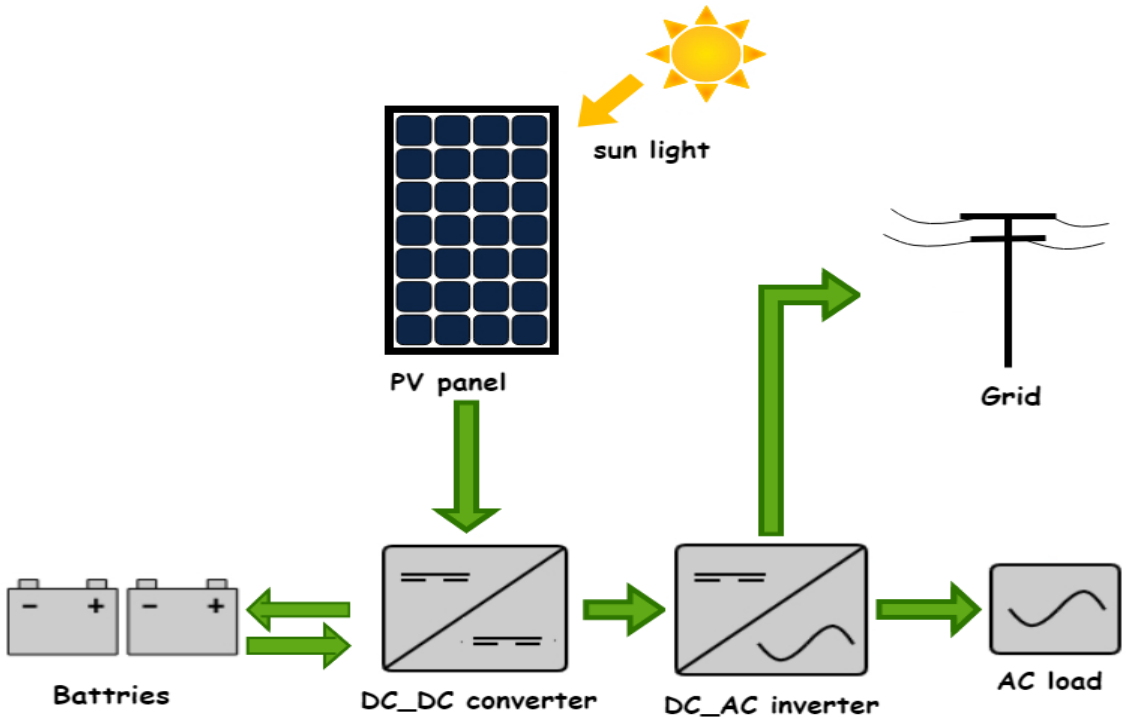

Figure I.2. A typical PV system.

Principally, PV systems can be divided into two categories according to their application:

- Stand-alone systems.
- Grid-connected systems.

I.3.1. Stand-alone system

Also known as off-grid PV power system, usually requires a storage battery, this type generally operates independently of the utility grid, designed and sized to supply certain DC and/or AC electrical loads. For DC load application, PV systems utilize single-stage DC-DC power converter, which plays a major role in changing the PV voltage or current level for tracking the maximum power point (MPP). For AC load application, a two-stage topology along with battery banks connected between the two stages is used. In the first stage, a DC-DC converter is used to boost the PV voltage and track the MPP. In the second stage, the DC-AC

inverter is utilized to convert the DC power to AC power and improve the AC power quality. In case of PV application with a critical load, battery banks are used to fix the inverter DC voltage and enhance or supply the required load power [6]. Figures I.3 show, respectively, the block diagram of the standalone PV system for DC and AC loads.

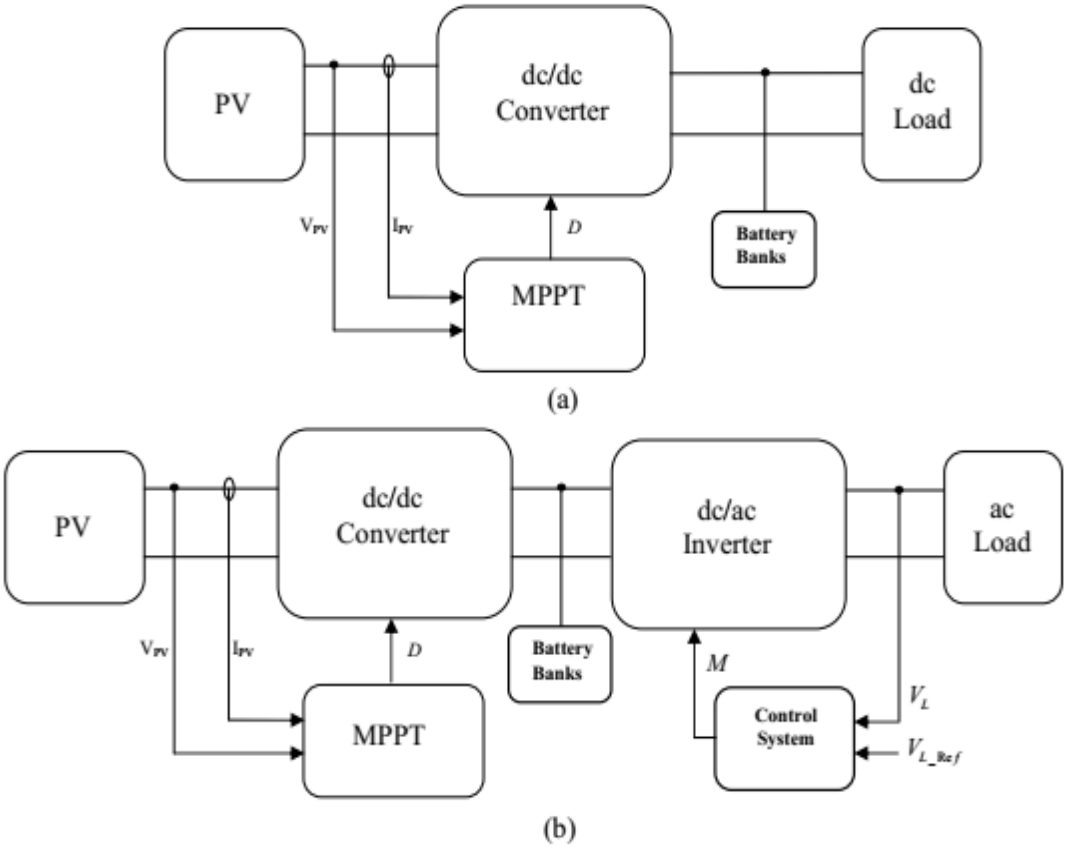

Figure I.3. Block diagram of standalone PV systems supplying (a) DC load and (b) AC load.

I.3.2. Grid-connected system

In order to inject the power generated by PV modules into the grid, it must be converted first from DC power to AC power. So, a power electronics inverter is employed. In addition to the converting capability, the inverter is used for the MPPT (Maximum power point tracking). Also, a DC-DC converter could be used to boost the PV output voltage and track the MPP. There are different inverter configurations [7]:

- Centralized technology.
- String technology.
- Multi-string technology.
- AC-module technology.

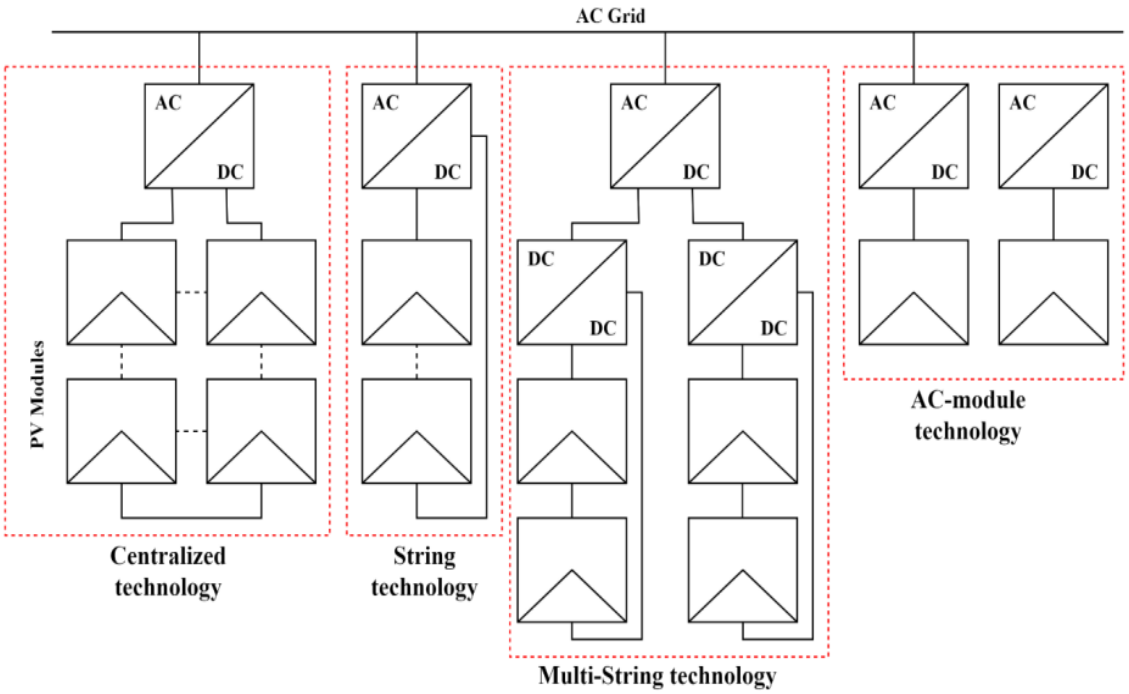

Figure I.4. Photovoltaic grid interfacing system technologies.

Figure I.4 shows the grid-connected PV system technologies, centralized inverter technology is considered the first PV grid-connected configuration, PV strings (a number of PV modules connected in series) are connected in parallel in order to obtain a PV array with the desired output power and DC voltage level. The PV array output is connected to a single DC to AC inverter. In this configuration, PV maximum power is delivered into the grid with high efficiency, small size, and low cost. Although, to fulfil grid requirements, such topology requires either a step-up transformer, which reduces the system efficiency and increases cost,or a PV array with a high DC voltage. A high voltage PV system suffers from hotspots (where a PV module with lower radiation behaves as a load) during partial shading and increased leakage current between the PV panel. Furthermore, the parallel connected PV strings could have different optimum voltages, resulting in multiple peaks on the PV array characteristic curve. To improve MPPT during partial shading or string optimum voltage mismatch, string technology is used, where each PV string is connected to an inverter with its own MPPT. This configuration has few drawbacks, it requires a large number of components and has high installation costs. The multi-string technology is similar to string technology. The difference is that a DC-DC converter is installed on each PV string where the outputs of each DC-DC converter are connected to a single DC-AC inverter. The added DC-DC converter on each string is employed to track the MPP and avoids having a large DC voltage PV module, this

technology is expensive because each string has its own converter. In AC-module technology, each PV module is connected to a different inverter, where the MPP from each module is extracted separately. This technology is recommended when PV modules with different power rating are used and it is considered the most expensive [7].

Besides, single and two stages grid-connected topologies are commonly used topologies in single and three-phase PV systems.

I.3.2.1. Single-stage grid-connected system

A single-stage grid-connected system is illustrated in Figure I.5. In order to track the MPP and interface the PV system to the grid, the PV system utilizes a single conversion unit (DC-AC power inverter). In such topology, PV maximum power is delivered into the grid with high efficiency, small size, and low cost. However, to fulfil grid requirements, this topology requires either a step-up transformer, which reduces the system efficiency and increases cost, or a PV array with a high DC voltage. High voltage systems suffer from hotspots during partial shading and increased leakage current between the panel, as described in section I.3.2. Furthermore, it is complicated to control the inverter because the control objectives such as MPPT, power factor correction and harmonic reduction. Different types of DC-AC inverters have been applied to enhance and regulate the performance, such as two-level and multilevel voltage source inverters and current source inverters [6].

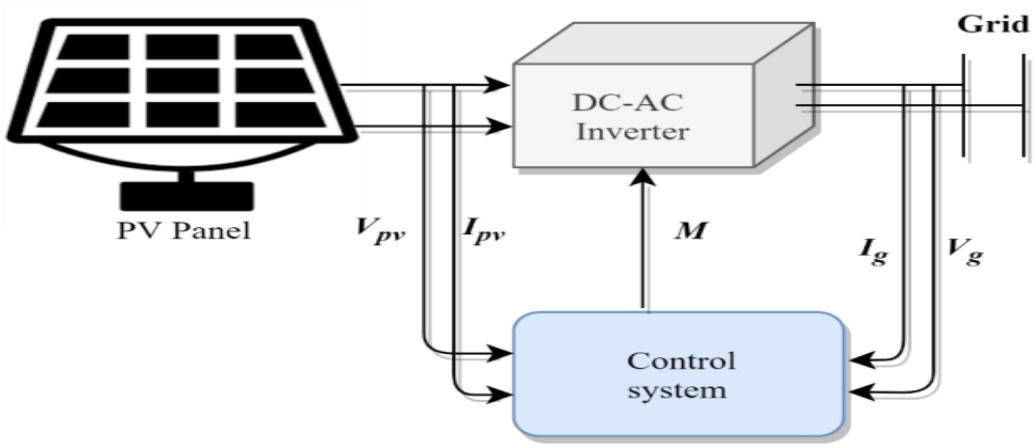

Figure I.5. Single stage grid-connected PV-system.

I.3.2.2. Two-stage grid-connected system

A block diagram of two stage grid-connected PV-system is presented in Figure I.6. The first stage is normally a DC-DC converter for extracting maximum power from the PV panel, the second one is a DC-AC converter for delivering power to the grid, and each of them is controlled in purpose of reducing load current ripple and keeping the output voltage level at

desired value. The advantages of the two-stage topology lie in the simplicity of designing the control scheme, since the control requirements are distributed between the two stages. Furthermore, a PV array with a high voltage output is not required because of the firstamplification stage. This topology suffers from higher power losses, larger footprint and higher cost than single-stage systems [6].

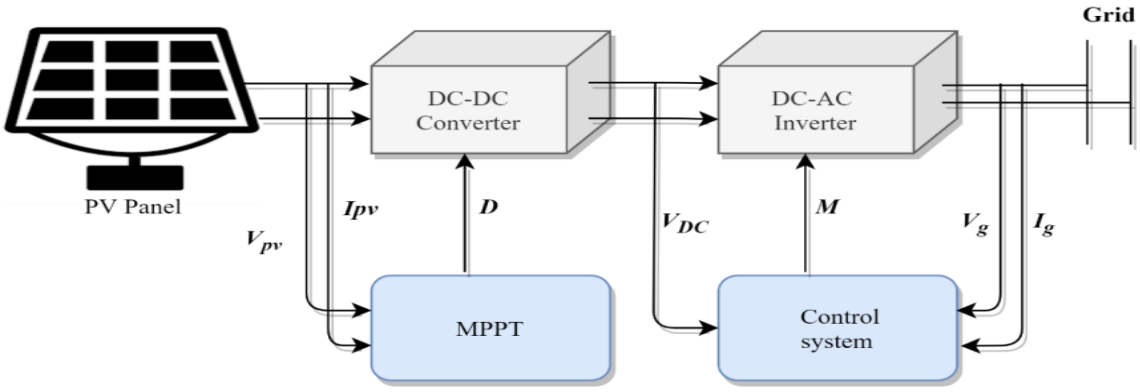

Figure I.6. Two-stage grid-connected PV-system.

I.4. Power electronics interfacing topologies for single-phase grid-connected PV systems

As presented before, two main configurations can be distinguished: single-stage PV systems and two-stage conversion systems. For the first configuration, a DC/DC converter is inserted between the PV source and the inverter. For the second, a DC-AC converter (inverter) is used for the conversion and transfer of PV power to the load or grid-connected.

I.4.1. DC-DC converters

As the name suggests, a DC-to-DC Converter is designed to convert one DC voltage into another DC voltage. They are used to increase or decrease the voltage level (Figure I.7). DC-DC converters are based on an electronic circuit that uses electronic switching technology. A DC-DC converter can support both very low voltage and high voltage applications [7].

DC-DC converters are mostly used in order to produce voltage that is regulated and consistent, arising from a source that is fluctuating or is not constant. These converters use high frequency switching circuit, together with inductors, switches, and capacitors in order to reduce the switching noise and maintaining regulated DC voltage. Even in the case that the input or output voltage may vary, DC to DC converters ensure a constant output in terms of the voltage thanks to closed feedback loops, thus maintaining its efficiency as a power conversion circuit [7].

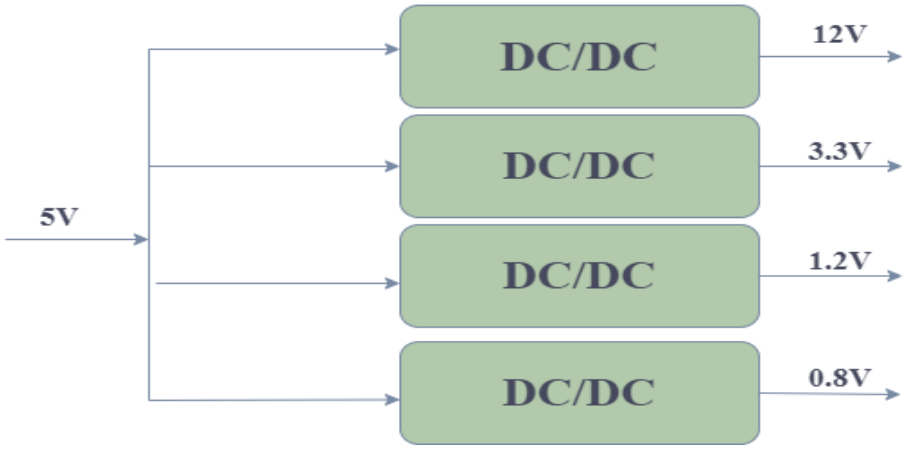

Figure I.7. DC-DC converters.

I.4.1.1. Types of DC-DC converters

There are many different types of DC-DC converters depending on the application they can be used for. The three main types are [7]:

a- **Buck converter:** is a DC-DC converter (Figure I.8) that is producing a voltage that has been stepped down (reduced) from the input voltage. This converter is suitable when the desired load voltage is less than the voltage corresponding to the MPP.

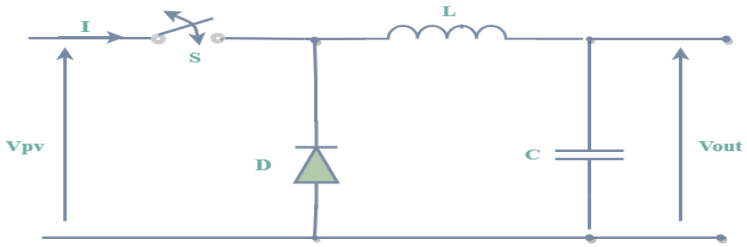

Figure I.8. Circuit diagram of Buck converter.

b- **Boost converter:** this type (Figure I.9) steps the voltage up as suggested by its name and thus produces a higher output voltage as opposed to the lower input voltage.

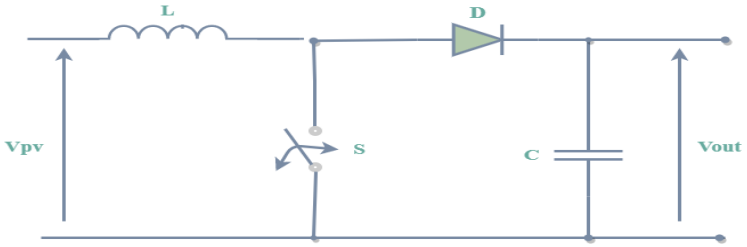

Figure I.9. Circuit diagram of Boost converter.

c- **Buck-Boost converter:** is a dual-purpose DC-DC converter, it can either step up or step down the voltage in order to produce an output that may be higher or lower than the input.

It can also be used to produce either negative or positive voltages and thus, is used in a variety of places.

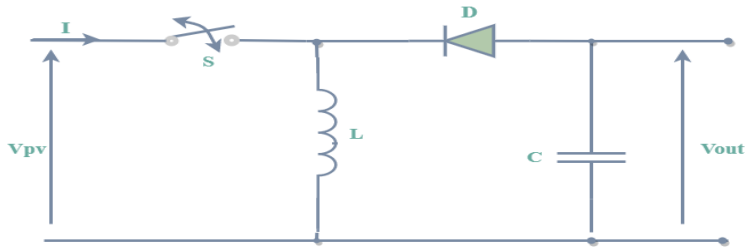

Figure I.10. Circuit diagram of Buck-Boost converter.

I.4.2. DC-AC converters

DC to AC converters is mainly designed for changing a DC power supply to an AC power supply. Here, DC power supply is comparatively stable as well as positive voltage source whereas AC oscillates approximately a 0V base stage, typically in a sinusoidal or square or mode.

I.4.2.1. Two-level single-phase inverter

An inverter is a DC-AC static converter, that is, an input DC voltage is converted into an output AC voltage. A Tow-level inverter consists of two switching cells structured in a H-bridge. The components traditionally used are IGBT with its antiparallel diode.

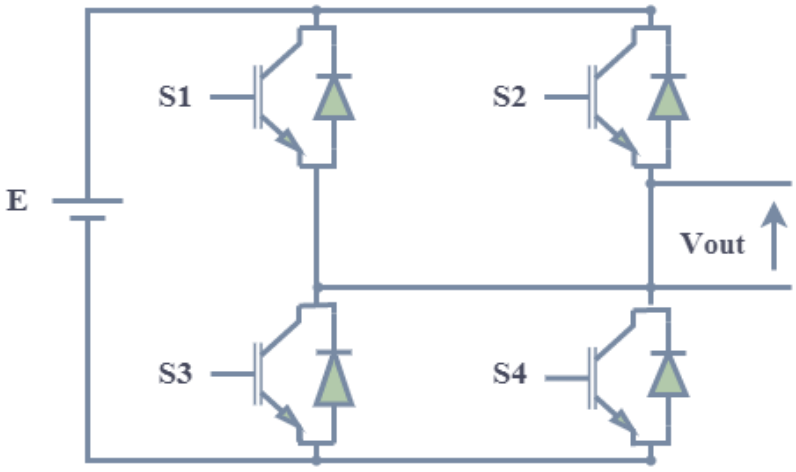

Figure I.11. Two-level single-phase inverter.

In order to avoid the short circuit across the DC input and the undefined AC output-voltage condition, the control technique should always ensure that at any instant either the top or the bottom switch of the inverter leg is on. The AC output voltage of the two-level single-phase inverter is depicted in Figure I.12.

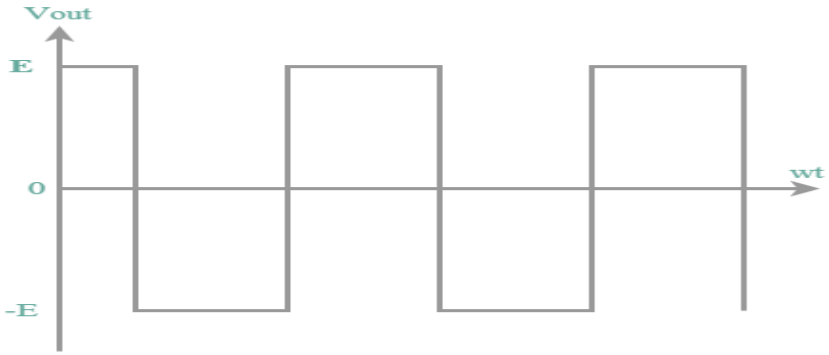

Figure I.12. The output voltage waveform of single-phase two-level inverter.

I.4.2.2. Multi-level single-phase inverter

Multilevel inverters have emerged as the most significant advancement over conventional converters; which could only produce a two-level voltage waveform at the output. The two-level waveform has a lot of harmonics, which needs the use of bulky filters to eventually generate a sinusoidal voltage waveform. Multilevel inverters can produce different voltage levels using combinations of switches and DC sources. The numerous levels reform the voltage waveform into a quasi-sine wave with low harmonic components. Therefore, the need of large filters to eliminate voltage harmonics is removed. On the other hand, dividing the voltage between switches makes it easier to use multilevel converters in high-power applications using only medium voltage switches [8].

Figure I.13(a) depicts a conventional inverter that can produce +E or –E at the output point with respect to the grounded neutral point, while Figure I.13(b) depicts a three-level inverter that produces +E, 0 and – E at the output, and Figure I.13(c) depicts a n-level inverter that generates multilevel voltages of 0, ± E, and ±2E….

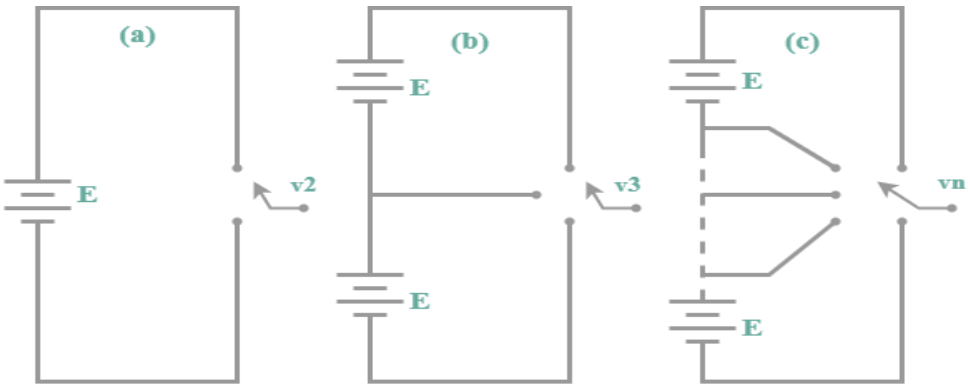

Figure I.13. One leg of, (a) 2-level, (b) 3-level and (c) n-levels inverter.

Due to its appealing qualities, multilevel inverters have lately attracted the attention of researchers and industry. The following are some of the most significant advantages of multilevel inverters:

- ❖ Reduced output voltage distortion due to various output waveform levels.
- ❖ Used for High power applications.
- ❖ Lower switching frequency results in lower switching losses.
- ❖ Low harmonic voltage/current waveforms.

For single-phase multilevel inverters, various topologies have been proposed, which are presented following:

a- Cascade topology: this topology can be used for medium and high-power applications; the cascade H-Bridge (CHB) multilevel inverter is most commonly utilized. The CHB is made up of numerous units of single-phase H-Bridge inverters connected in series. The output voltage levels, depending on the number of DC sources, will be able to range from *-mE* to *mE*, with *2m + 1* levels. Where *m* is the number of distinct DC sources. Increasing the number of levels results in a virtually sinusoidal output voltage waveform. Even without applying any filters, increasing the number of levels causes the output voltage waveform to become almost sinusoidal. Figure I.14 illustrates a single-phase five-level CHB, which contains two single-phase HB cells. In this case, the five output voltage levels are 0, ±E, and ±2E, which are shown in Figure I.15 [8].

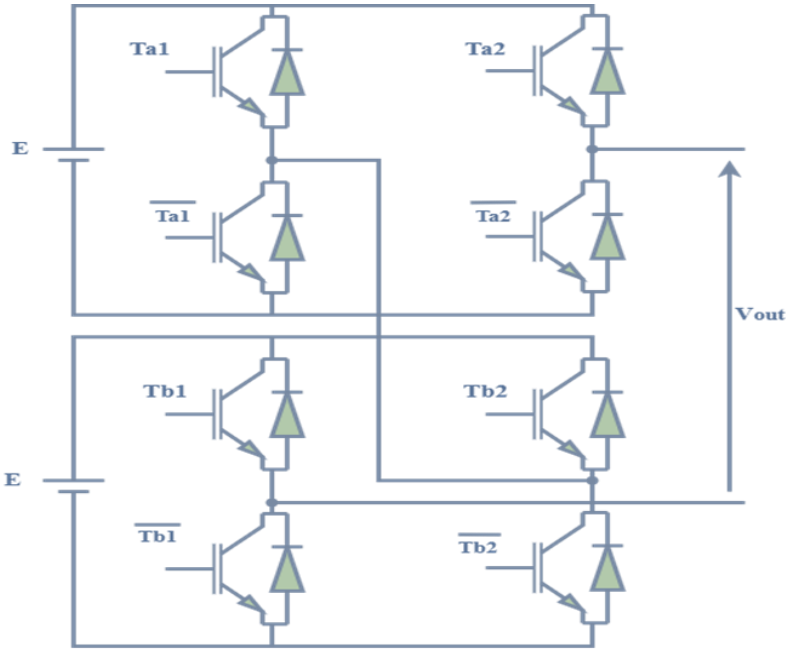

Figure I.14. Single-phase five-level CHB inverter.

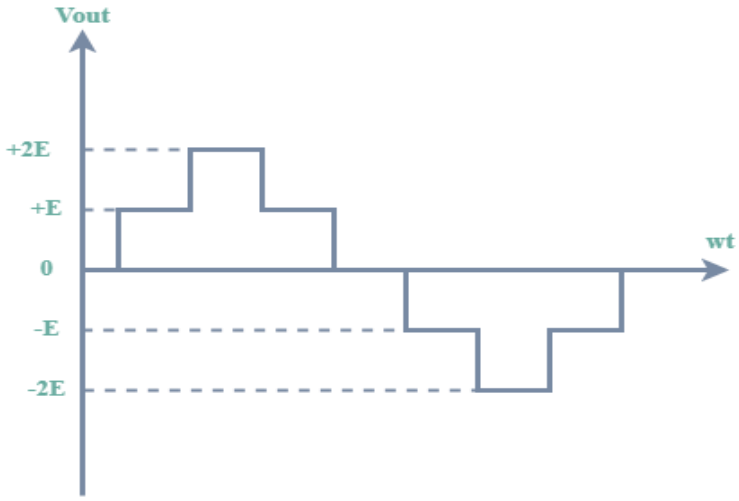

Figure I.15. The output voltage waveform of single-phase five-level CHB inverter.

The output voltage levels of the single-phase inverter CHB are listed in Table I.1. The main disadvantage of this topology is the high cost of the inverter, because increasing the number of voltage levels necessitates a large increase in the number of switches and DC sources.

Table I.1. Switching states for five-level CHB Inverter.

Switching sequences				Voltage levels
Ta1	Ta2	Tb1	Tb2	Vout
0	1	0	1	-2E
0	1	0	0	-E
0	0	0	0	0
1	0	0	0	+E
1	0	1	0	+2E

b- **Neutral-point clamped topology:** Figure I.16 depicts a five-level single-phase neutral point clamped (NPC) inverter, initially proposed by Nabae, Takahashi et Akagi, 1981. After that, the five-level NPC has found many developments and usage in industries. The clamped diodes (D1a, D2a, D1b, and D2b) are connected to the DC capacitors neutral points, resulting in a zero-level addition to the output voltage. In this topology, clamping diodes play a very important role in keeping the switch voltage at the necessary level. The switching state of a five-level NPC inverter is shown in Table I.2. One of the advantages of this structure is its flexibility to be controlled using both PWM and space vector modulation

(SVM) [8]. Nevertheless, when the number of voltage levels is very large, the system is hard to construct given a large number of semiconductors necessary (the number of clamping diodes can be written as (*m-1*) (*m-2*), where *m* is the number of levels).

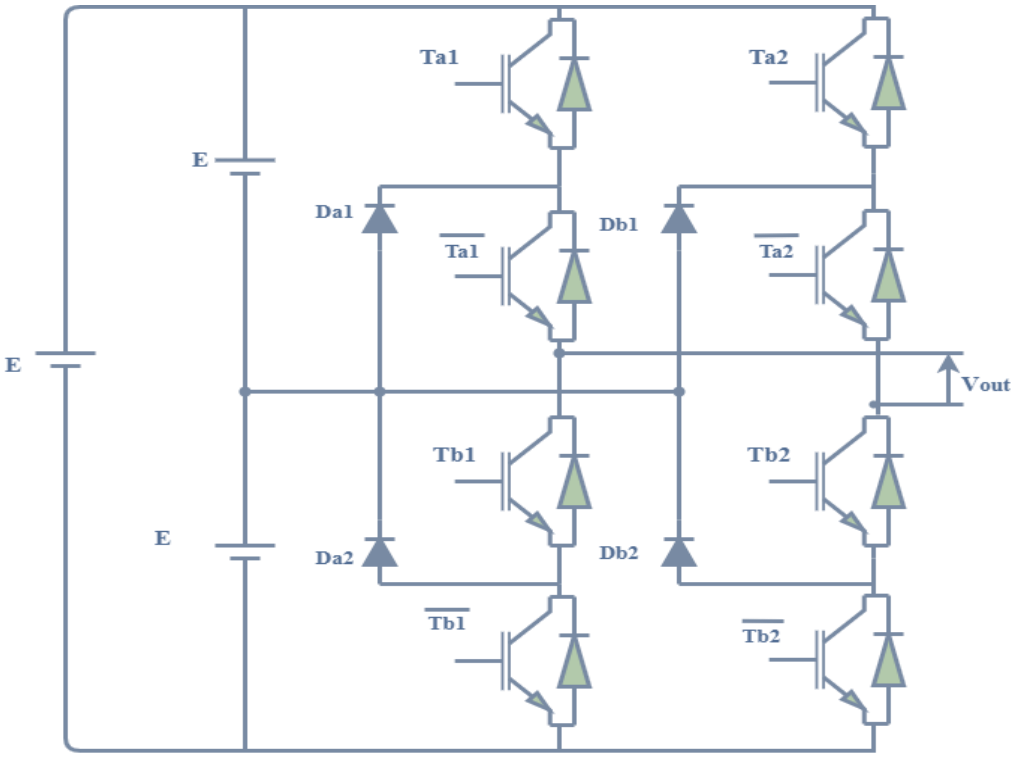

Figure I.16. Single-phase five-level NPC inverter.

Table I.2. Switching states for Diode-Clamped Multilevel Inverter.

Switching sequences				Voltage levels
Ta1	Ta2	Tb1	Tb2	Vout
1	1	0	0	+E
0	1	0	0	+E/2
0	0	0	0	0
0	0	0	1	-E
0	0	1	1	-E/2

c- **Flying capacitors topology:** the flying capacitor (FC) topology is also another multilevel inverter topology proposed by Escalante Vannier and Arzandé, 2002. Figure I.17 presents the topology of three-level FC inverter. This topology has a similar number of switches as the NPC multilevel inverter, but the number of additional capacitors beyond the primary

DC-bus capacitors is (*m-1*) (*m-2*)/*2*, where *m* is the number of levels. In addition, it needs a high number of isolators for DC capacitors, as well as a complicated voltage balancing control, limiting its practical application. Table I.3 lists the switching state of a three-level FC inverter [8].

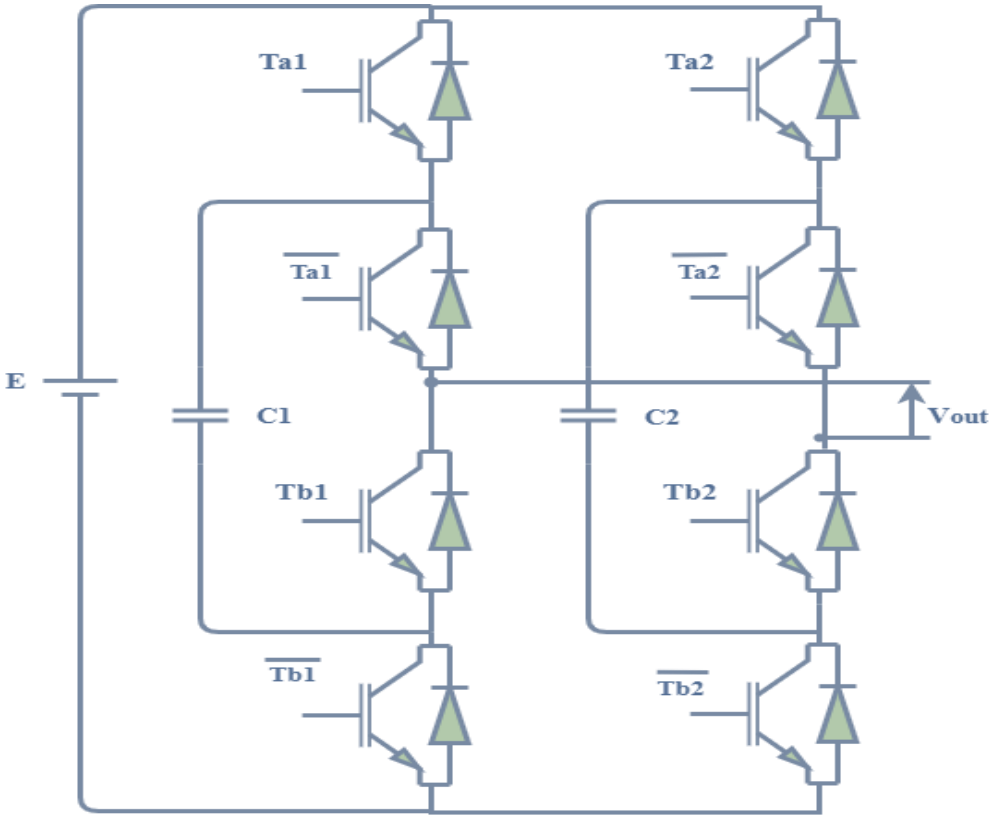

Figure I.17. Single-phase three-level FC inverter.

Table I.3. Switching states for three-level FC Inverter.

Switching sequences				Voltage levels
Ta1	Ta2	Tb1	Tb2	Vout
1	1	0	0	+E
1	0	1	0	0
0	0	0	0	0
0	1	0	1	0
0	0	1	1	-E

d- **Packed U cell topology:** this topology is a hybridization of FC and CHB with less capacitors and semiconductors. Al-Haddad introduced the PUC converter in 2011, and Vahedi

developed it in 2015. It can be utilized in both single-phase and three-phase configurations. Packed U cells as shown in Figure I.18, each U cell is made up of two power switches and a capacitor. The benefits of the proposed concept will be confirmed in the next chapter by simulation results and experimental validation.

Figure I.18. Single packed U cell.

I.4.2.3. Comparison between different single-phase multilevel inverter topologies

Following the brief descriptions of multilevel inverter topologies, a brief conclusion based on comparative analysis can be given, as shown in Table I.4.

Table I.4. Single-phase multilevel inverter components.

.n: Celle .m: number of levels				
Topology	NPC	FC	CHB	PUC
Source DC	(m-1)	1	(m-1)/2	1
No. of clamping diodes	2(m-2)	0	0	0
No. antiparallel diode	2(m-1)	2(m-1)	2(m-1)	$2^{\log_2(m+1)}$
No. of switches	2(m-1)	2(m-1)	2(m-1)	$2^{\log_2(m+1)}$
No. of capacitors	0	(m-2)	0	$\log_2(m+1)-1$
Total Number	7m-9	5(m-1)	(9/2)(m-1)	-

Based on comparison study, a short conclusion can be formulated after the conducted brief descriptions related to multilevel inverter topologies, as shown in Table I.5. In comparison to the other topologies, PUC5 has achieved reliability and lower cost.

Table I.5. Comparison between five-level inverter topologies.

Configuration	NPC	FC	CHB	PUC
Source DC	4	1	2	1
No. of clamping diodes	6	0	0	0
No. antiparallel diode	8	8	8	6
No. of switches	8	8	8	6
No. of capacitors	0	7	0	1
Total Number	26	20	18	14

I.5. Control objectives of grid-connected PV photovoltaic systems

As shown in Figure I.19, the control objectives of a grid-connected PV system can be divided into two major parts: (1) PV-side control with the purpose to maximize the power from PV panels and (2) grid-side control performed on the PV inverters with the purpose of fulfilling the demands to the grid. In order to maximize the power, it is important to track the most extreme power point of the PV generator. PV system has a single operating point that can give maximum power to the load. This point is called the maximum power point (MPP). Hence, to function the PV generator at its greatest power point, distinctive algorithms can be utilized such as perturb and observe (P&O), Incremental Conductance (IncCon) which are very popular because of their simplicity and fast convergence. In addition, there are other intelligent algorithms as fuzzy control, genetic algorithms …etc. But they have some drawbacks, including complex implementation and difficulties in initial point selection. On the other side, different control strategies are also applied in a closed-loop for a photovoltaic inverter to generate a gating pulse signal such as direct power control (DPC) and the reference current extraction methods. In the last methods, a PI controller is used to regulate the DC-link voltage and estimate the amplitude of the reference grid currents. It should be noted that the injected grid current is demanded to be synchronized with the grid voltage, different methods to extract the grid voltage information have been developed in recent studies like the zero-crossing method, the filtering of grid voltage method, and the phase-locked loop (PLL) techniques, which give the best performance. PLL is a feedback control system used to generate an output signal when the phase is related to the phase of input signal, only if frequency, voltage and phase are the same, it creates an output signal [9].

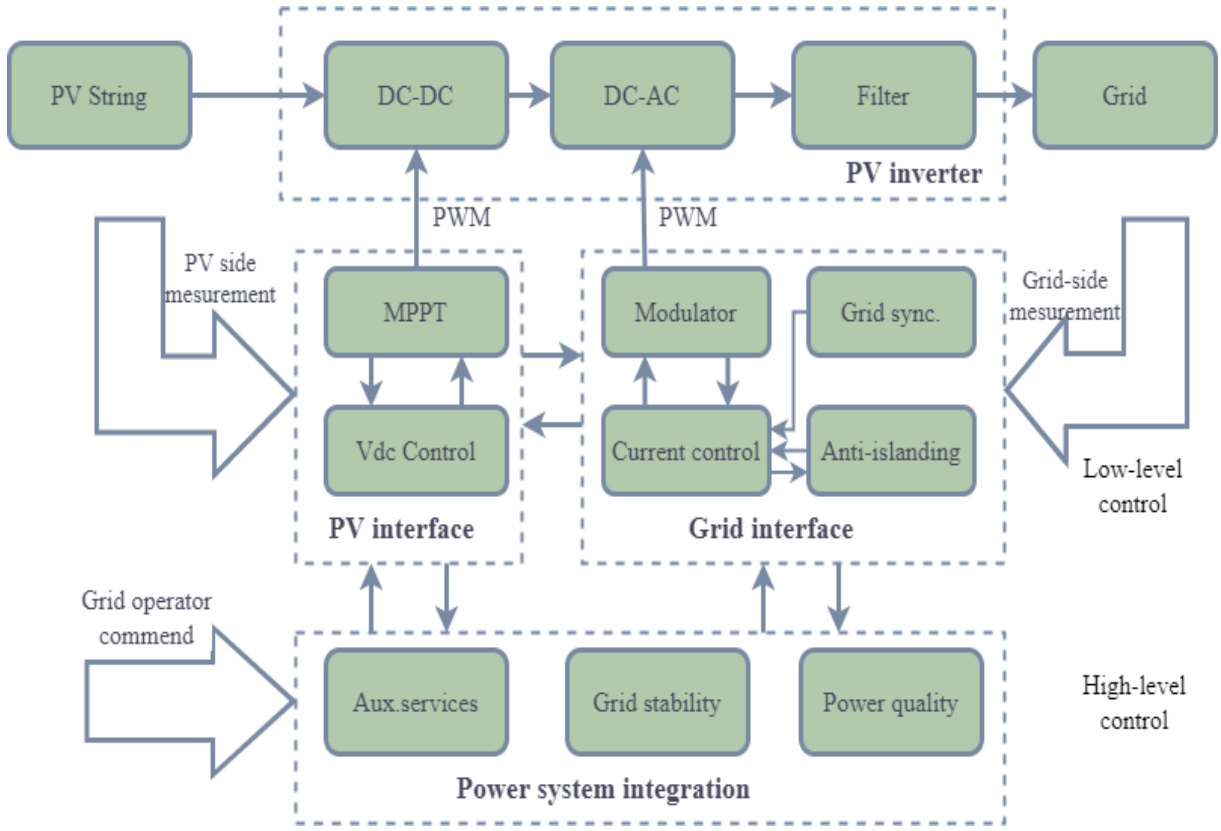

Figure I.19. General control blocks (control objectives) of a grid-connected PV system**.**

I.6. Conclusion

In this chapter, an overview on single-phase grid-connected PV systems is presented. Stand-alone and grid-connected PV systems were described to show their power circuit and control schemes. The integration options for a grid-connected PV system were discussed to explain their power electronics topology requirements. The most common topologies of the DC-DC and DC-AC converters, which are used on either single, or two stage topologies were discussed and compared. In addition, the general control objectives for grid-connected PV systems are presented.

The next chapter will focus on the modeling and the control of a grid-connected PV system based on multi-level single-phase inverter.

Chapter II:

Modeling and Control of a Single-Phase Grid-Connected PV System using PUC5 Inverter

II.1. Introduction

Following the discussion in the previous chapter, a typical configuration of a single-phase grid-connected photovoltaic (PV) system, shown in Figure II.1, is a promising solution for an effective, economic and robust PV grid-connected system. The system includes a PV generation

system, which is a group of series-parallel connected modules (PV array). A passive input filter, a capacitor, which is used to reduce the current and voltage ripple (and hence power) at the PV side, follows the PV array. The input filter is followed by a DC-DC boost converter, which is used to perform the maximum power point tracking (MPPT) of the PV array and elevate its voltage. The DC-DC converter is connected through DC-link (capacitor) to the single-phase 5-level packed U cells (PUC) inverter. The inverter is used to convert the DC power to AC power and feeds the energy to the utility grid with high power quality.

In this chapter, a single-stage grid-connected PV system based on a 5-level PUC inverter is presented and molded. In addition, an effective control scheme based on advanced technique ‘’Model predictive control’’ for the presented grid-connected PV system is developed.

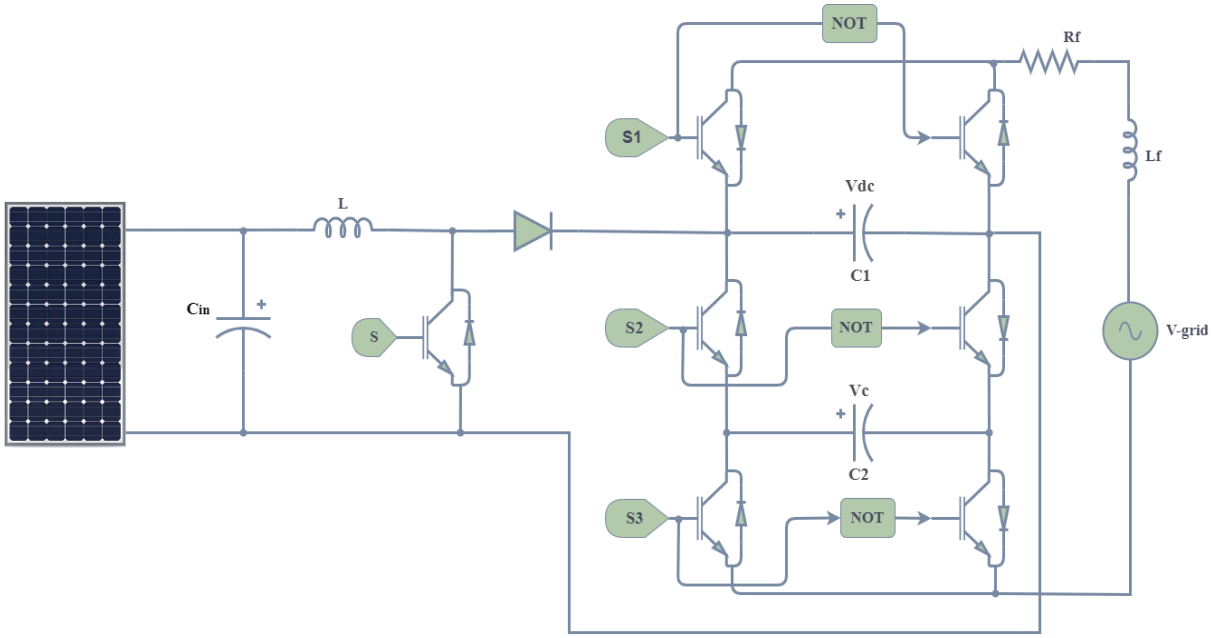

Figure II.1. Block diagram of the proposed PV grid-connected system.

II.2. Photovoltaic panel modeling

In general, PV cells are combined in series and in parallel, before being enclosed in a glass envelope to get a photovoltaic module.

A PV panel consists of modules linked together (Figure II.2) to form a unit capable of delivering high continuous power, suitable for domestic or industrial PV applications [10, 11].

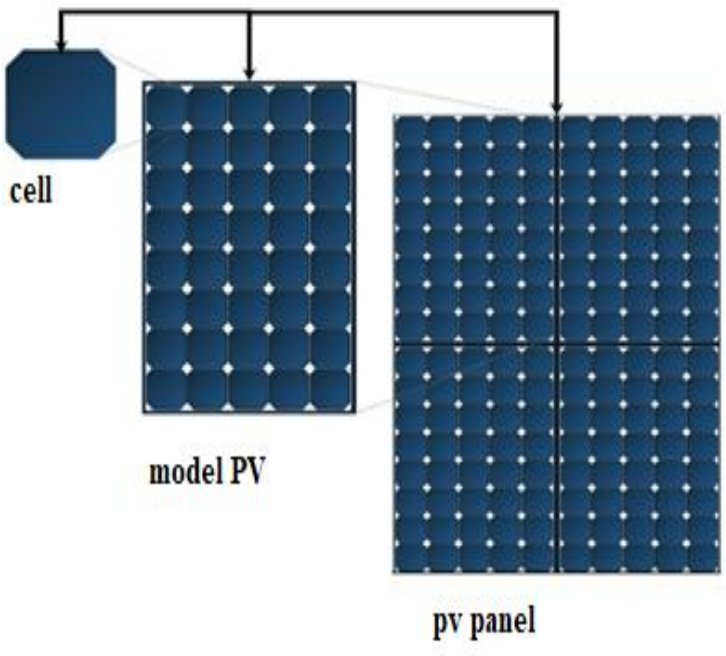

Figure II.2. Constitution of a PV panel.

II.2.1 Model of the photovoltaic cell

A PV cell is modeled in the literature by several circuits. The most commonly used equivalent circuit of a PV cell is composed of a current source in parallel with a diode, a shunt resistor R_{sh} and a series resistor R_s (Figure II.3) [10].

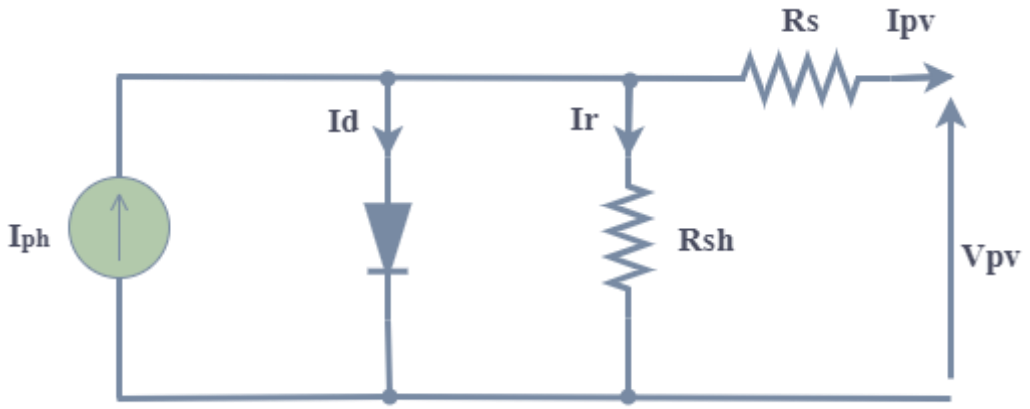

Figure II.3. Equivalent circuit diagram of a PV cell.

The output current of the cell is given by the following equation:

$$I_{PV} = I_{ph} - I_d - I_r = I_{ph} - I_o\left(e^{\frac{V_{PV}+R_I I_{PV}}{nV_t}} - 1\right) - \frac{V_{PV} + R_s I_{PV}}{R_{sh}} \qquad \text{(II.1)}$$

Where:

I_{PV} : is the output current of the cell [A].

I_{ph} : is the photo-current of the cell [A], proportional to the illumination given by:

$$I_{ph} = \left(I_{sc,STC} + K_i(T - T_{STC})\right)\frac{G}{G_{STC}} \qquad \text{(II.2)}$$

With:

$I_{sc,STC}$: is the court-circuit current under standard test conditions (STC) [A].

K_i : is the temperature coefficient of the court-circuit current, normally provided by the manufacturer.

T : is the temperature of the cell [°K].

T_{STC} : is the temperature of the cell at STC (298.15°K).

G : is the solar irradiance incident on the surface of the cell [W/m²].

G_{STC} : is the illuminance in STC conditions (1000 W/m²).

I_r: is the current derived by the shunt resistor [A].

I_d: is the current of the diode [A].

I_o: is the reverse saturation current of the diode [A], described as follows:

$$I_o = I_{o,STC}\left(\frac{T_{STC}}{T}\right)^3 e^{\left[\frac{qE_g}{nk}\left(\frac{1}{T_{STC}}-\frac{1}{T}\right)\right]} \quad \text{(II.3)}$$

Where:

$I_{o,STC}$: is the reverse saturation current of the diode under STC conditions, expressed as:

$$I_{o,STC} = \frac{I_{sc,STC}}{e^{\left(\frac{V_{oc,STC}}{nV_{t,stc}}\right)}} \quad \text{(II.4)}$$

$V_{oc,STC}$: is the open circuit voltage under STC conditions [V].

$V_{t,STC}$: is the thermal voltage under STC conditions (0.02569 V).

n : is the ideality factor of the diode (Coefficient depending on the material of the PV cell, generally PV cell, in general: 1 < n < 2).

E_g: is the Gap energy of the cell (crystalline silicon Eg = 1.12 eV)

k: is the Boltzmann constant (1.38 x 10-23 J/°K

q : is the electric charge (1.6 x 10-19 C)

V_{PV} : is the output voltage of the cell [V].

V_t: is the thermal voltage [V], given by:

$$V_t = \frac{kT}{q} \quad \text{(II.5)}$$

II.2.2. Photovoltaic module model

The model presented previously concerns a single PV cell, for the module model it is necessary to integrate number of cells in parallel/series, forming a module. Figure II.4 shows the equivalent circuit of a PV module. Thus, the PV module current is expressed by [11]:

$$I_{PV} = N_p I_{ph} - N_p I_o\left(e^{\frac{N_s V_{PV}+(N_s/N_p)R_s I_{PV}}{nN_s V_t}} - 1\right) - \frac{N_s V_{PV} + (N_s/N_p)R_s I_{PV}}{(N_s/N_p)R_{sh}} \quad \text{(II.6)}$$

Where:

I_{PV}: is the output current of the module [A].

V_{PV} : is the output voltage of the module [V].

N_s: is the number of cells connected in series per module.

N_P: is the number of cells connected in parallel per module.

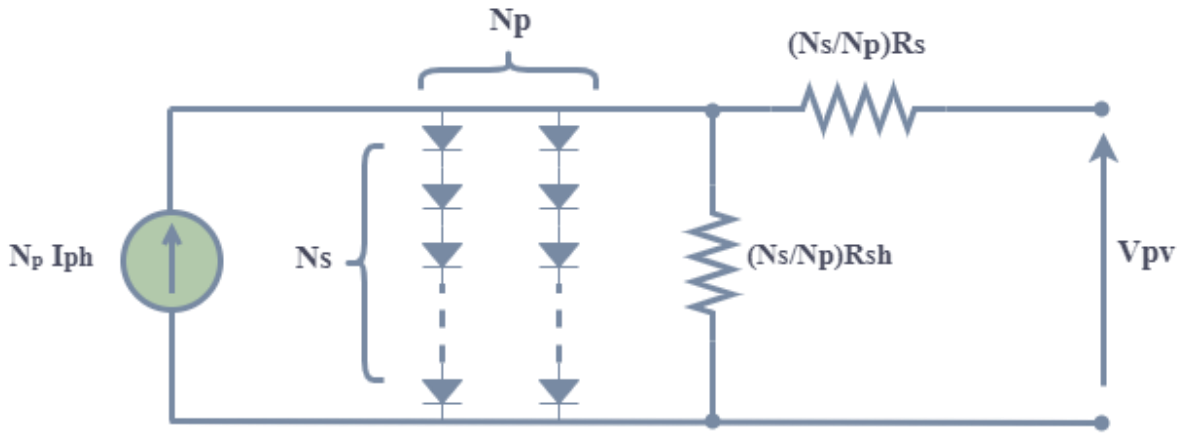

Figure II.4. Equivalent circuit diagram of a PV module.

The characteristics of a PV module are presented in (Figure II.5).

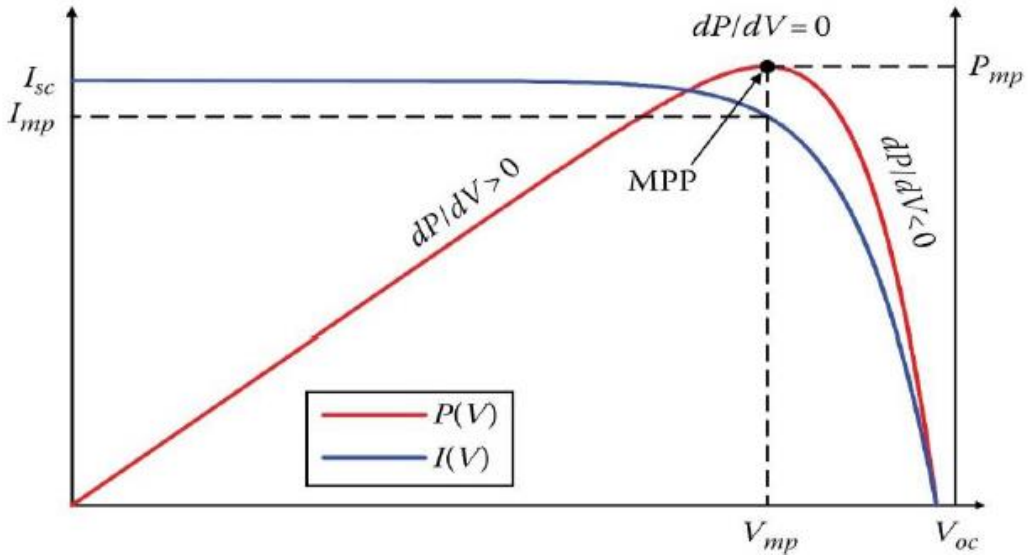

Figure II.5. Characteristics of a PV module.

In Figure II.5, there are three remarkable points [10, 11]:

- The short-circuit point $(0,\ I_{sc})$: (i.e., the point where the I-V curve meets the voltage axis), where I_{sc} is the court-circuit current that can be measured by connecting the positive and negative terminals of the PV modules. It corresponds to the highest value of the current generated when the voltage is zero.
- The open circuit point $(V_{oc},\ 0)$: (i.e., the point where the I-V curve meets the axis of curent), where V_{oc} is the open circuit voltage of the PV module. It represents the voltage of the module in the dark. In this case, no current is generated.

- The maximum power point, MPP (V_{mpp}, I_{mpp}): In this case, the PV module said that the PV is operating in the optimum efficiency and providing a maximum power P_{mpp} given by:

$$P_{mpp} = I_{mpp}V_{mpp} \quad \text{(II.7)}$$

With:

I_{mpp} and V_{mpp} are respectively the optimal values of the current and voltage of the PV module.

In addition, two important parameters of the PV module can also be defined:

- The form factor FF: it is the report of the maximum power that can be extracted when we product $I_{sc}V_{oc}$:

$$FF = \frac{P_{mpp}}{I_{sc}V_{oc}} = \frac{I_{mpp}V_{mpp}}{I_{sc}V_{oc}} \quad \text{(II.8)}$$

- The conversion efficiency: it's the report of the maximum electrical power that can be extracted from the incident radiation power G on the surface Sr of the PV module:

$$\eta = \frac{P_{mpp}}{\mathrm{Sr}\,G} = \frac{I_{mpp}V_{mpp}}{\mathrm{Sr}\,G} = \frac{I_{sc}V_{oc}FF}{\mathrm{Sr}\,G} \quad \text{(II.9)}$$

II.2.3. Photovoltaic panel model

A PV panel consists of a number of PV modules connected in series/parallel to obtain the desired voltage, current and power. The size of a panel changes from a single module to another number of modules. The output current and voltage of a PV panel can be calculated from the following equations:

$$I_{PVt} = N_{pp}I_{PV} \quad \text{(II.10)}$$

$$V_{PVt} = N_{ss}V_{PV} \quad \text{(II.11)}$$

Where:

I_{PVt}: is the output current of the panel [A].

V_{PVt} : is the output voltage of the panel [V].

I_{PV} : is the output current of the module [A].

V_{PV} : is the output voltage of the module [V].

N_{ss} : is the number of modules connected in series per panel.

N_{pp} : is the number of modules connected in parallel per panel.

II.3. POWER converters modeling

II.3.1. Boost converter model

The boost converter is a voltage booster. Figure II.6 shows an equivalent circuit of a typical boost converter, which consists of a diode, an electronic switch (IGBT), an inductor L and a capacitor C . The capacitor functions as a filter to improve the quality of charging voltage [12].

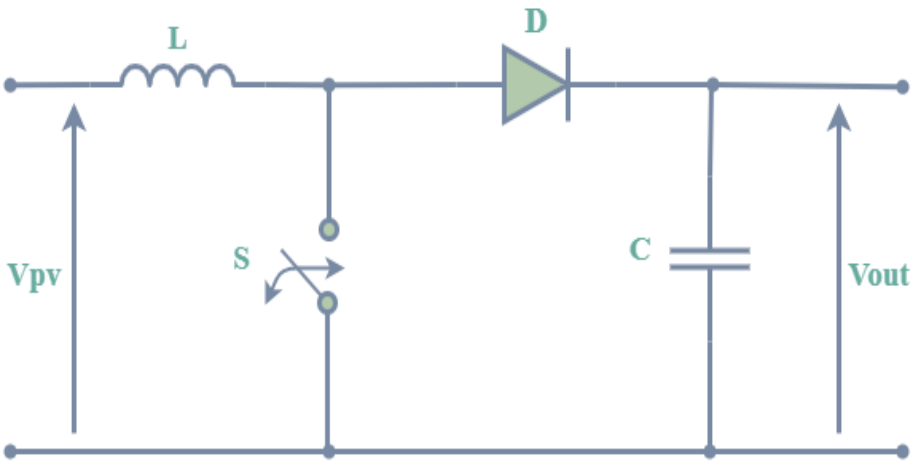

Figure II.6. The boost converter circuit.

The modelling of this converter goes through the analysis of the different operating sequences that we will assume of durations fixed by the command S. During the operation of the boost, the switch will be switched at a frequency f_c with a closing time equal to DT_c and an equal opening time $(1-D)T_c$. Two operating sequences therefore appear depending on the state of the switch (Figure II.7), each of which we can represent by a differential equation:

- When the switch is closed $t \in [0 \;\; DT_c]$:

$$\begin{cases} \frac{d}{dt} I_L = \frac{1}{L} V_{PV} \\ \frac{d}{dt} V_C = -\frac{1}{C} I_{\text{out}} \end{cases} \quad \text{(II.12)}$$

- When the switch is open $t \in [DT_c \;\; T_c]$:

$$\begin{cases} \frac{d}{dt} I_L = \frac{1}{L} (V_{PV} - V_C) \\ \frac{d}{dt} V_C = \frac{1}{C} (I_L - I_{\text{out}}) \end{cases} \quad \text{(II.13)}$$

By multiplying equations (II.12) and (II.13) by DT_c and $(1-D)T_c$ respectively, we obtain the dynamic boost model:

$$\begin{cases} \frac{d}{dt} I_L = \frac{1}{L} V_{PV} - (1-D)\frac{1}{L} V_C \\ \frac{d}{dt} V_C = (1-D)\frac{1}{C} I_L - \frac{1}{C} I_{out} \end{cases} \quad \text{(II.14)}$$

Where:

I_L : is the boost input current [A]

V_{PV} : is the boost input voltage [V]

V_C : is the boost output voltage [V]

I_{out} : is the boost output current [A]

T_c : is the switching period of the boost (which is equal$1/f_{ct}$) [s]

D: is the duty cycle ($D \in [0 \ \ 1]$).

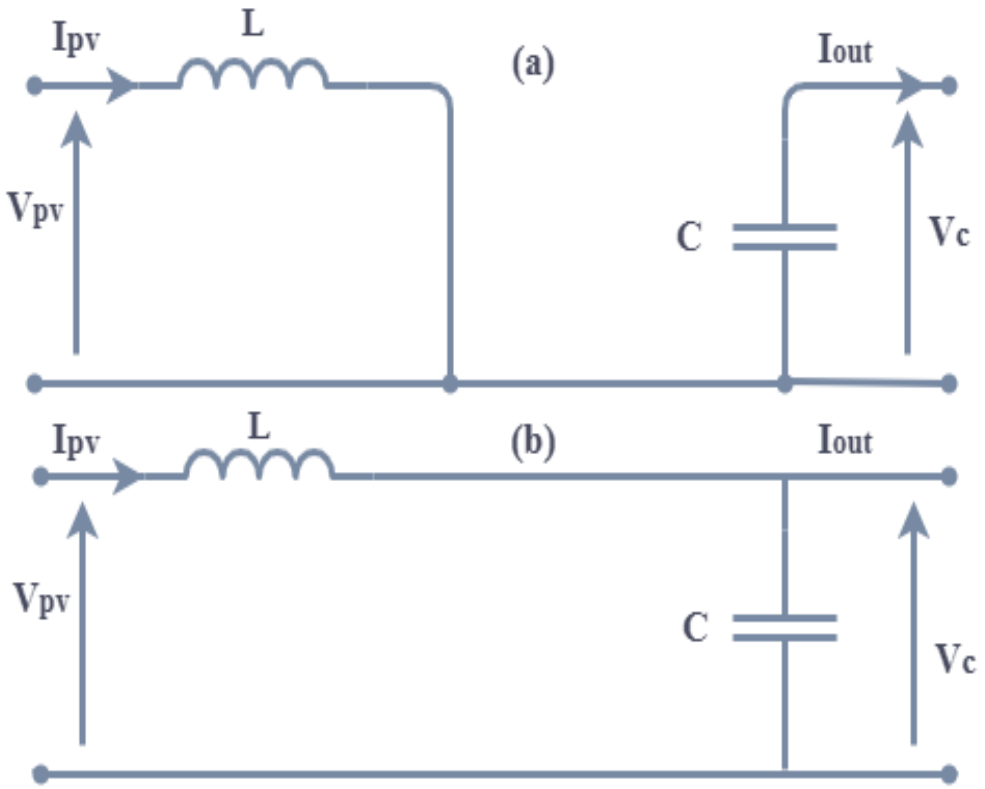

Figure II.7. (a) when the switch is closed; (b) when the switch is open.

II.3.2. PUC5 converter model

PUC5 inverter structure has been shown in Figure II.8. It is made of six active switches and two DC links. Each pair of switches (S_1&S_4, S_2&S_5, S_3&S_6) is working complementarily. Each two switches are connected to a DC bus as U-Cell and these cells build the whole PUC converter. As an inverter application, the higher DC link would be an isolated DC source (or a

PV panel) and the lower DC link is a capacitor which its voltage should be controlled and regulated [13].

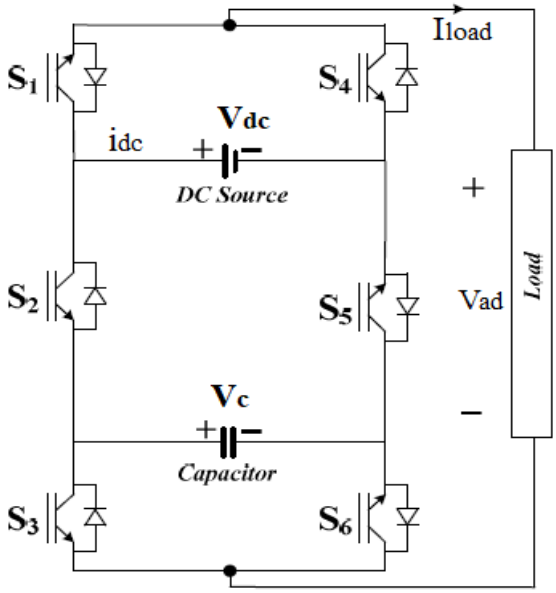

Figure II.8. PUC5 topology.

Table II.1: PUC5 capacitor voltage states.

State	S_1	S_2	S_3	Output voltage (V_{ad})	Capacitor voltage
1	0	0	0	V_{dc}	No effect
2	0	0	1	$V_{dc} - V_c$	Charging
3	0	1	0	V_c	Discharging
4	0	1	1	0	No effect
5	1	0	0	0	No effect
6	1	0	1	$-V_c$	Discharging
7	1	1	0	$-V_{dc} + V_c$	Charging
8	1	1	1	$-V_{dc}$	No effect

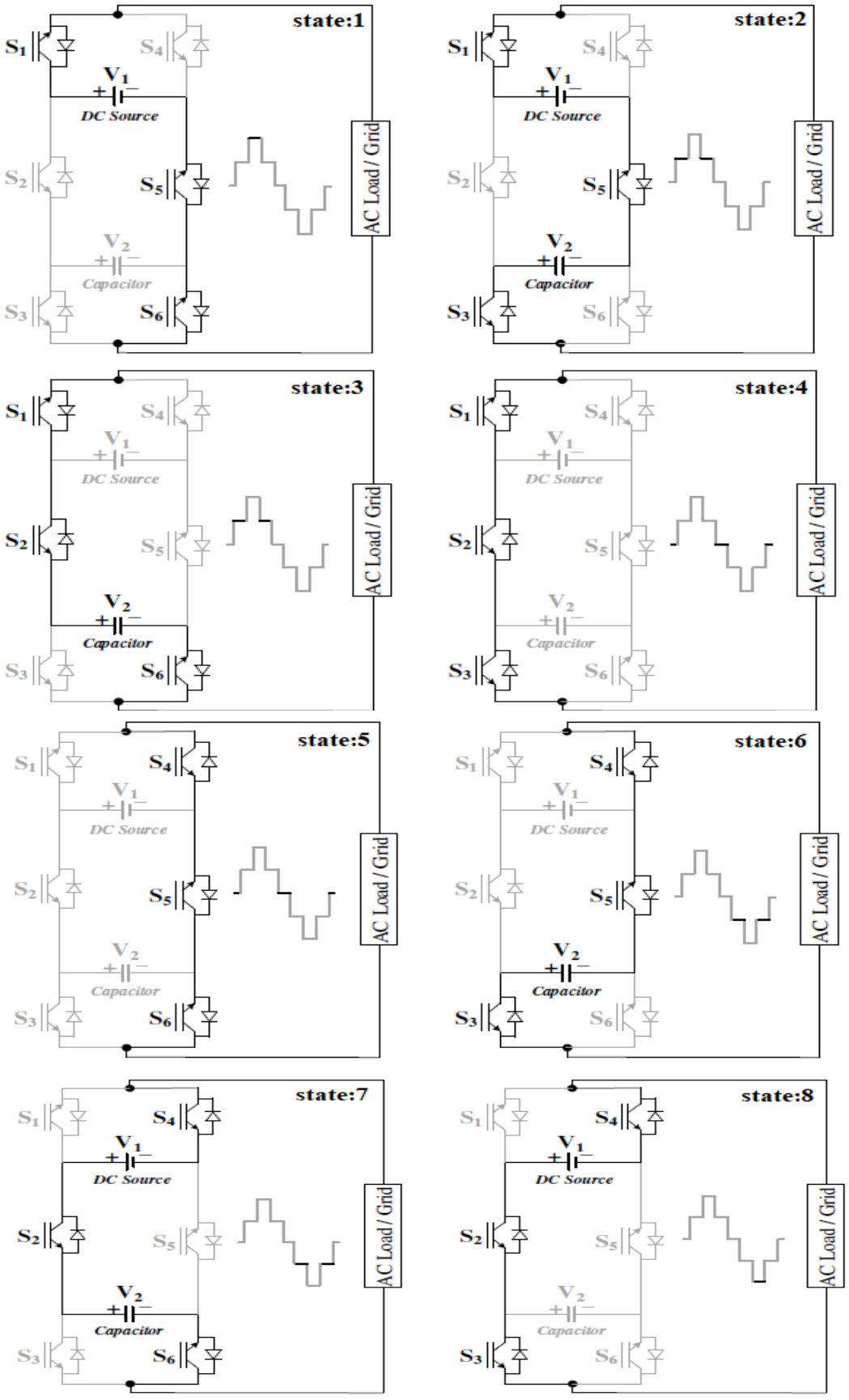

FigureII.9. Switching states of PUC5 inverter.

II.4. Suggested control scheme

The complete control scheme for the studied PV grid-connected system is shown in Figure II.10. In this scheme, the MPPT is applied to track the maximum power from the PV panel using a method called P&O (Perturbation and observation). Phase Locked Loop (PLL) block ensures that both grid current and voltage are synchronized, and the PI controller regulates the DC-link voltage and estimate the amplitude of the reference grid current. MPC algorithm based on PWM bloc controls the PUC5 inverter by providing proper switching signals.

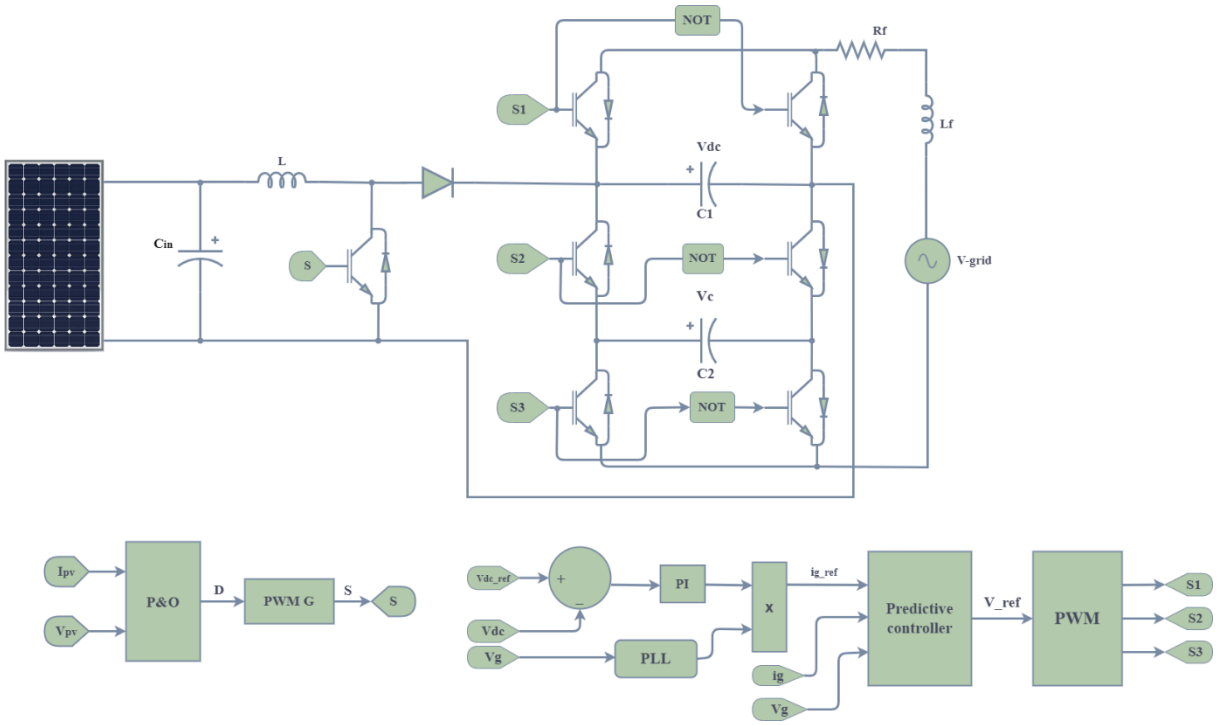

Figure II.10. Suggested control scheme for the studied PV grid-connected system.

II.4.1. Maximum power point tracking

MPPT is one of the essential functions in PV systems. Considering the nonlinear current–voltage characteristics of PV panel, the maximum power delivered by the PV array is at a well-defined operating point named maximum power point (MPP). MPPT is one of the key functions that every grid connected PV inverter should have. There is a large number of publications dealing with MPPT, where the majority of the PV converters are able to extract around 99% of the available power from the PV installation, over a varied irradiance and temperature range in steady and dynamic states.

The most frequently applied MPPT algorithms are hill-climbing methods, such as the perturb and observe (P&O), and its alternate implementation (with identical behavior), the incremental conductance. The P&O technique is the most popular MPPT algorithm for industry applications due to the good balance between complexity, accuracy and reliability. The P&O

method is based on the property that the derivative of the power–voltage characteristic of the PV panel is positive on the left side and negative on the right side (see Figure II.5), while at the MPP, it holds that $\Delta Ppv > 0$. During the execution of the P&O MPPT process, the output voltage and current of the PV panel are periodically sampled at consecutive sampling steps in order to calculate the corresponding output power and the power derivative with voltage. The MPPT process is performed by adjusting the reference signal of the DC/DC power converter PWM controller. Figure II.11 presents the flowchart of the P&O MPPT [12].

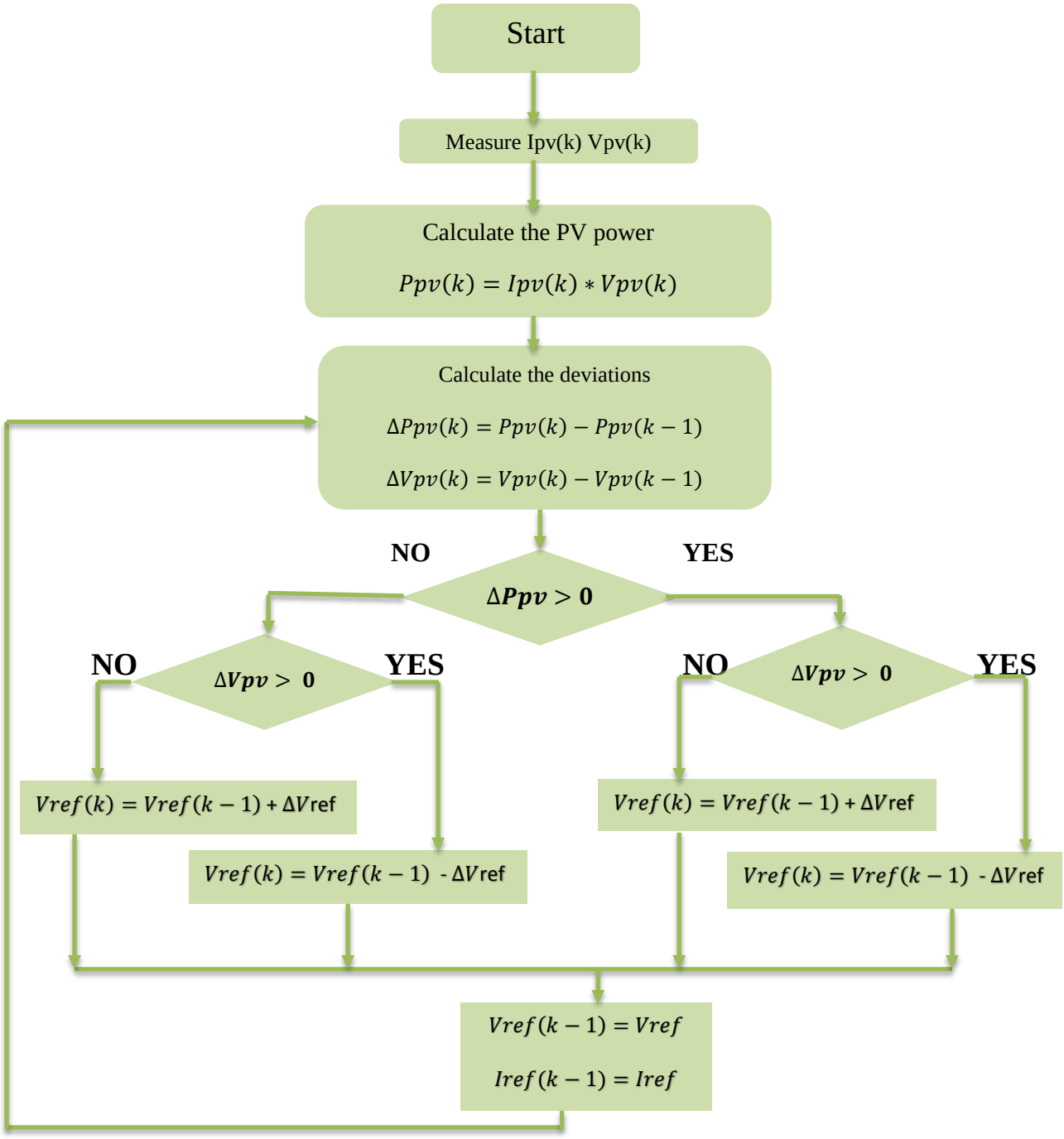

Figure II.11. Flowchart of P&O MPPT algorithm.

II.4.2. DC-link voltage controller

To reduce the DC-link capacitor fluctuation voltages and compensate the system loss regarding the power exchange between the PV system and main grid, a proportional-integral (PI) controller is used to decrease to voltage fluctuation in the DC-link, and regulate it at a desired value. Figure II.12 shows the synaptic of the PI controller, when the input is the error between the DC-link capacitor voltage V_{dc} and the estimation value V_{dc_ref}, the output of the regulator is the amplitude of the reference grid current I_{g_ref} [16 14].

Figure II.12: PI DC-link voltage controller.

The PI controller can be modelled as a second-order system as fellow [16 14]:

$$\frac{V_{dc}}{V_{dc\_ref}} = \frac{k_p s + k_i}{C_1 s^2 + k_p s + k_i} = \frac{\frac{k_p}{C_1}s + \frac{k_i}{C_1}}{s^2 + \frac{k_p}{C_1}s + \frac{k_i}{C_1}} \qquad \text{(II.15)}$$

The transfer function is a second order transfer function and the characteristic equation can be expressed as:

$$s^2 + \frac{k_p}{C_1}s + \frac{k_i}{C_1} = s^2 + 2\xi\omega_n s + \omega_n^2 \qquad \text{(II.16)}$$

So, the gain k_i and k_p can be expressed as:

$$k_p = 2\xi\omega_n C_1 \qquad \text{and} \qquad k_i = C_1\omega_n^2 \qquad \text{(II.17)}$$

Where: ξ is the damping coefficient ($\xi = 0.707$) and ω_n is the natural frequency$\left(\omega_n = 2\pi \times 25\frac{rad}{s}\right)$.

II.4.3. Grid synchronization

In PV grid-connected systems, the injected grid current should be synchronized with the grid voltage as required by the standards in this field. As a result, grid synchronization is an essential grid-monitoring task that will strongly contribute to the dynamic performance and the stability of the entire control system. The grid synchronization is even challenged in single-phase systems, as there is only one variable (the grid voltage) that can be used for synchronization. Nevertheless, different methods to extract the grid voltage information have

been developed, like the zero-crossing method, the filtering of grid voltage method, and the phase-locked loop (PLL) techniques, which are important solutions.

Figure II.13 shows the structure of the PLL-based synchronization system used in this work. It can be observed that the PLL system contains a phase detector (PD) to detect the phase difference, a PI-based loop filter (PI-LF) to smooth the frequency output, and finally a voltage-controlled oscillator (VCO) [16 14].

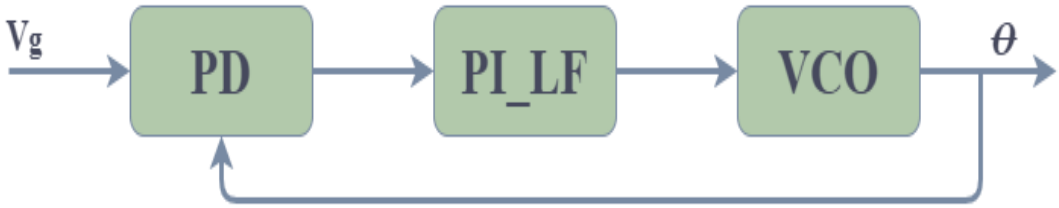

Figure II.13. Structure of the used PLL system.

II.4.4. Suggested MPC algorithm

The general model of a grid tie inverter can be written in terms of dynamic equations as (II.18), where L_g is the grid line filter with $R_g$as the parasitic and wiring resistance, i_g represents the grid line current, v_g is the grid voltage and V_{inv} is the PUC5 output voltage:

$$L_g \frac{di_g}{dt} = -R_g i_g + V_{inv} - v_g \qquad \text{(II.18)}$$

The aim of the controller is to regulate the grid line current through a predictive algorithm. For these reasons, a discrete-time model has to be taken into considerationT_s. is the system sampling time used in Euler-Forward approximation. Thus, the current derivative can be written as:

$$\frac{di_g(t)}{dt} \approx \frac{i_g(k+1)-i_g(k)}{T_s} \qquad \text{(II.19)}$$

The discrete-time grid current can be then written in equation II.20, where h denotes the prediction horizon:

$$\begin{aligned} i_g(k+h) = &\left(1 - \frac{R_g T_S}{L_g}\right) i_g(k+h-1) \\ &+ \frac{T_S}{L_g}\left(V_{inv}(k+h-1) - v_g(k+h-1)\right) \end{aligned} \qquad \text{(II.20)}$$

The main problem finite control set model predictive control is the variable switching frequency operation. This work solves this issue through applying a recently introduced optimization method to regulate the current injected by PUC5 topology. This latter takes in action of generating the optimum vector responsible of minimizing a cost function, which is

the same vector that nullifies its derivative. Therefore, calculating the general formula of this vector in terms of system parameters and giving it in each iteration will ensure that the cost function in each iteration is at its minimum and then, the errors between the state variables and their references is null. Considering the one-step prediction horizon, the single-phase predicted grid current can be written in terms of other variables as:

$$i_g^{\mathrm{p}}(k+1) = \left(1 - \frac{R_g T_S}{L_g}\right) i_g(k) + \frac{T_S}{L_g}\left[V_{inv}(k) - v_g(k)\right] \tag{II.21}$$

The proposed predictive algorithm only regulates the current so the cost function can be written as equation II.22, where i_{g_ref} is the reference amplitude of the grid current. Moreover, it should be noted that there is no need of defining a weighting factor since one state is controlled thanks to the sensor-less voltage balancing of the capacitor.

$$G = \left(i_{g\_ref} - i_g\right)^2 \tag{II.22}$$

Substituting equation II.22 in II.21 results in the following equation;

$$G = \left(\left(i_g^*(k+1) - \left\{1 - \frac{R_g T_S}{L_g}\right) i_g(k) - \frac{T_S}{L_g}\left[V_{inv}(k) - v_g(k)\right]\right)^2 \tag{II.23}$$

The aim of the algorithm is to generate the optimum output voltage V_{inv} that can be given to any modulator. Therefore, the task is to solve equation II.24.

$$\frac{\partial G}{\partial V_{inv}} = 0 \tag{II.24}$$

The derivative of $G(V_{inv})$ can be written as:

$$\partial G / \partial V_{inv} = -2\frac{T_S}{L_g}\left[\left(\left(i_g^*(k+1) - \left(1 - \frac{R_g T_S}{L_g}\right) i_g(k) - \frac{T_S}{L_g}\left[V_{inv}(k) - v_g(k)\right]\right)\right] \tag{II.25}$$

Solving equation II.25 gives II.26:

$$V_{inv,min} = -\frac{L_g}{T_S} A$$
$$A = \left(1 - \frac{R_g T_S}{L_g}\right) i_g(k) + \frac{T_S}{L_g} v_g(k) - \left(i_g^*(k+1)\right) \tag{II.26}$$

Studying the slope of the cost function derivative is a mandatory task to ensure an optimization process. As it is clear, the slope of the derivative given in equation II.25 is $\frac{-2T_S}{L_g}$ which is certainly negative. Thus, a minimum voltage generation is guaranteed. An overall schematic diagram of the proposed MPC controller is given in Figure II.14. In each single iteration, the controller reads the measured grid current and voltage given by sensors, then calculates the term A according to the desired current reference. It generates the vector $V_{inv,min}$ at final step, which is given in equation II.26 [14 15]. In our study, one-step prediction horizon was adopted to calculating the desired reference $i_{g_{ref}}(k+1)$ as equation II.27.

$$i_{g\_ref}\ (k\ +\ 1)\ =\ 3\ i_{g\_ref}\ (k)\ -3\ i_{g\_ref}(k-1)\ +\ i_{g\_ref}\ (k-2) \quad \text{(II.27)}$$

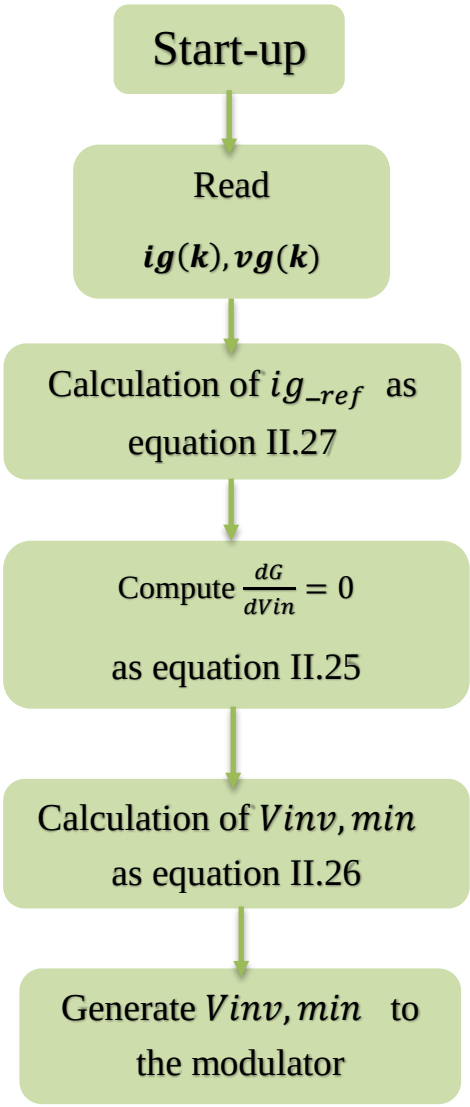

Figure II.14. Schematic diagram of the proposed MPC controller.

II.4.5. Pulse width modulation (PWM)

The general concept of a pulse width modulator (PWM) is that the reference voltage is compared to a triangular carrier signal and the output of the comparator is used to drive the single-phase multilevel inverter switches. Figure II.15 shown level-shifted PWM, that concept differs from other methods in a small way, for PUC5 inverter, 4 carrier wave would be compared by sinusoidal wave, and the four carrier's waveforms (Cr1, Cr2, Cr3, and Cr4) are shifted vertically to modulate the reference waveform V_{ref} completely, which generating a pulsed voltage waveform at the output of the inverter.

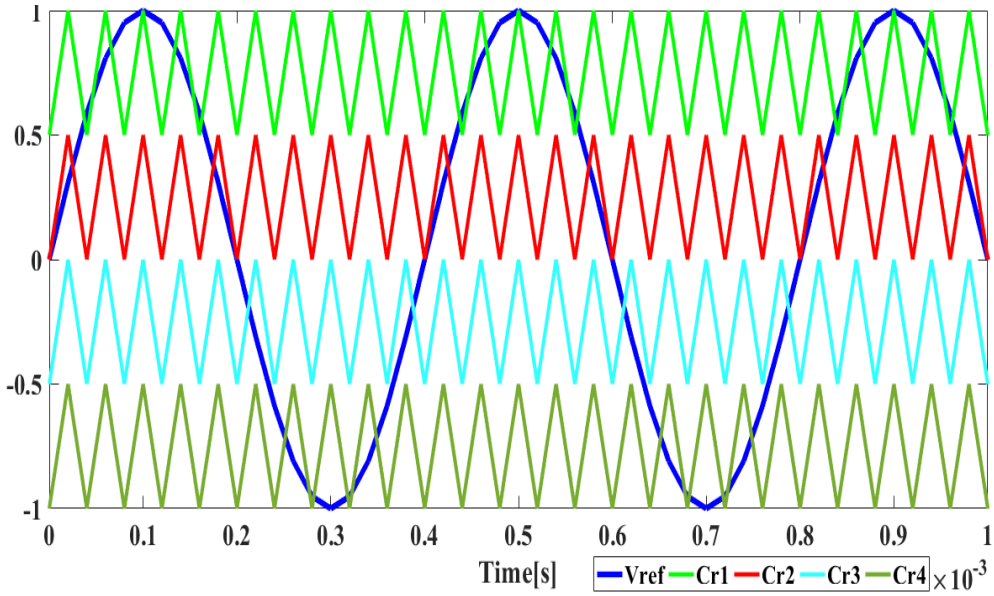

Figure II.15. Level shifted PWM carriers for PUC5 inverter

The firing pulses associated with switching states 1, 2, 4, 5, 6 and 8 (listed in Table II.1) are generated based on comparing V_{ref} with those carrier waves. Moreover, redundant switching states of 4 and 5 are used to reduce the switching frequency. If V_{ref} is positive, then state 4 will be used to produce the zero level at the output. On the other hand, if V_{ref} is negative, the output zero level voltage will be generated by state 5. The described algorithm is shown in Figure II.16, which can produce the five-level voltage waveform at the output with minimum switching frequency while fixing the capacitor voltage at the desired level without any feedback sensor [16].

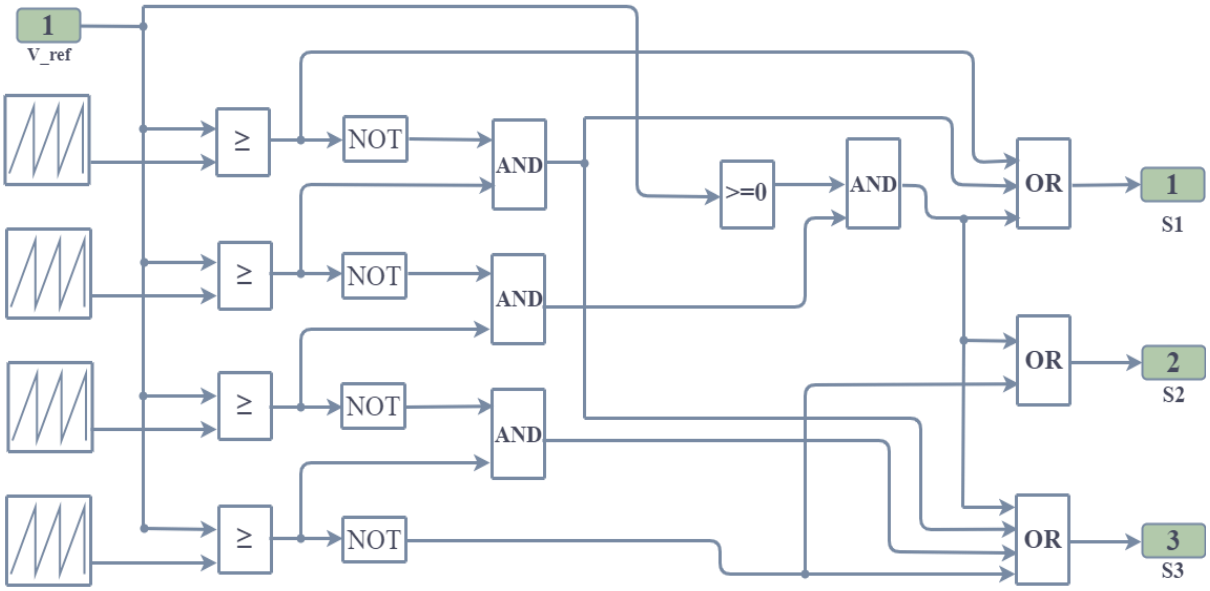

.

Figure II.16. Pulse width modulator for PUC5 inverter.

II.5. Simulation results

A simulation prototype of a single-phase grid-connected PV system based on PUC5 inverter has been implemented under MATLAB/Simulink in order to check the studied algorithms. The system simulation circuit is shown in the Figure II.17. The PV array consists of four PV modules (1Soltech 1STH-215-P) connected in a 2 (series) x 2 (parallel). PV module parameters are shown in Table II.2. Figures II.18 and II.19 illustrate current-voltage (I-V) and power-voltage (P-V) characteristics of the PV module. The system consists also of a boost converter, a PUC5 inverter and a utility grid which is modelled as a sinusoidal voltage source in series with a resistance and an inductance, an MPPT control to extract the Maximum power from the PV array, a PI controller to control the DC-link voltage, an MPC algorithm with PWM bloc to control the PUC5 inverter. The system contains also current and voltage sensors. The electrical parameters of the single-phase grid-connected PV system based on PUC5 are listed in Table II.3.

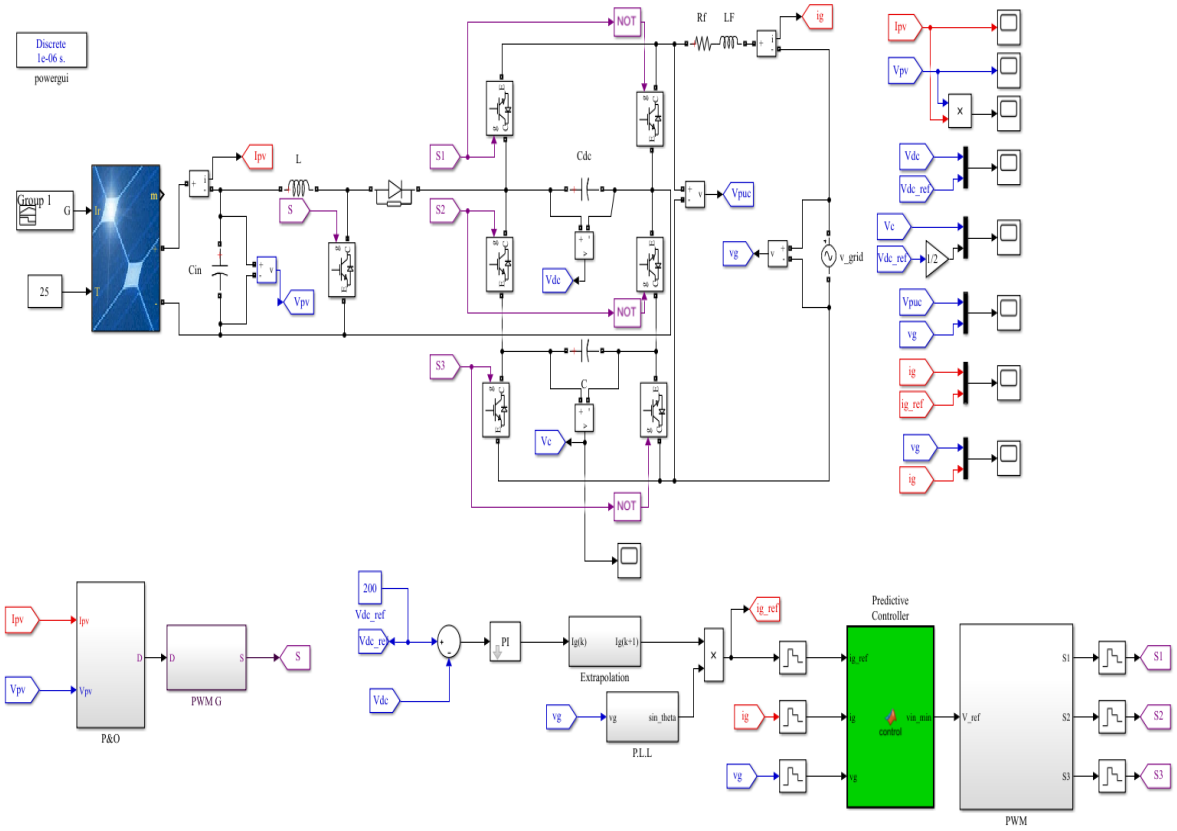

Figure II.17. Schema block diagram of the developed simulation.

Table II.2. PV module parameters.

PV Array	Values
Open circuit voltage (V_{oc})	36.3 V
Optimum operating voltage (V_{mpp})	29 V
Short circuit current (I_{sc})	7.84 A
Optimum operating current (I_{mpp})	7.35 A
Maximum power (P_{mpp})	213.15W
Temperature coefficient of V_{oc}	-0.36099 %/C°
Temperature coefficient of I_{sc}	0.102 %/C°
Cell per module (N_{cell})	60

Table II.3. Electrical Parameters of the single-phase grid-connected PV system using PUC5 inverter.

Component	Nominal value
Grid filter resistance (R_g)	0.1 Ω
Grid Filter inductance (L_g)	4 mH
Grid peak voltage (V_{g_max})	120 V
Grid frequency (f)	50 Hz
PUC5 DC capacitor1 (C_2)	2200 µF
PUC5 DC capacitor2 (C_2)	2200 µF
PV input capacitor (C_{PV})	1100 µF
Inductance Boost (L)	1 mH
Switching frequency of the Boost	2 Khz
Switching frequency of the PUC5	10 Khz

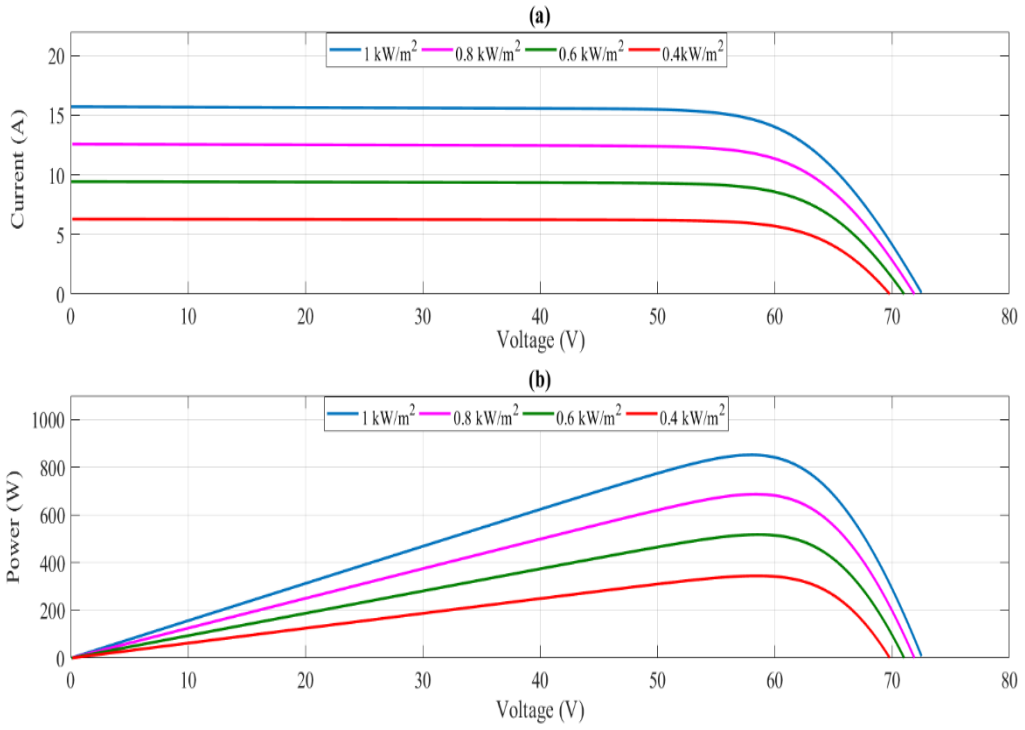

Figure II.18. Current-voltage (a) and power-voltage (b) characteristics of the PV array for different irradiance levels.

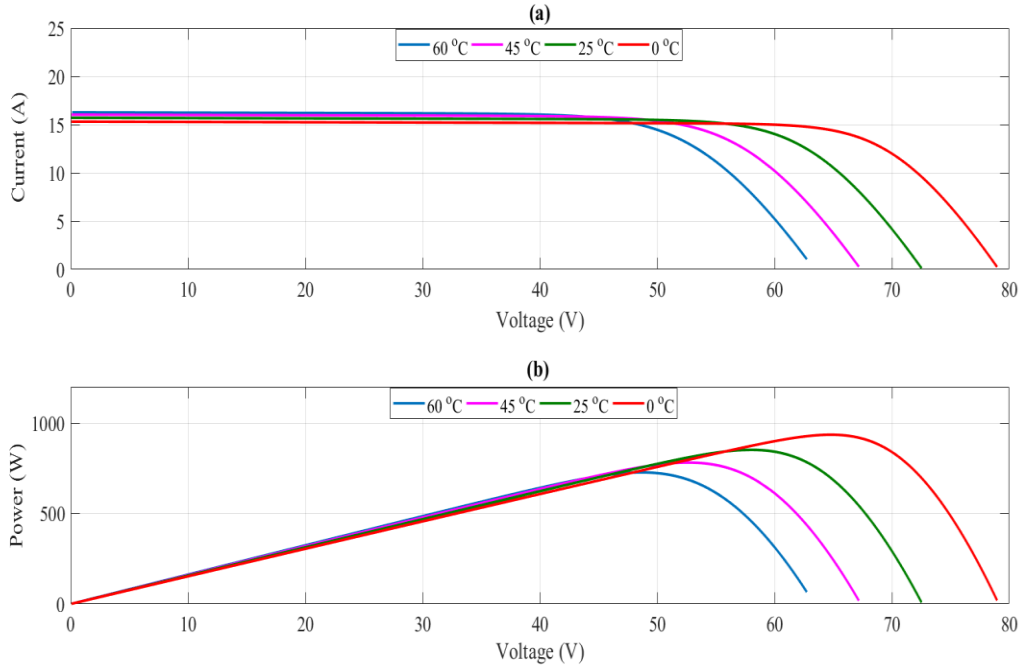

Figure II.19. Current-voltage (a) and power-voltage (b) characteristics of the PV array for different temperatures

An irradiance profile with various sudden irradiance change is applied to exam the suggested control system (Figure II. 20). Figures II.21-23 show the simulation results for voltage, current, and power outputs of the PV panel. It can be seen that the P&O algorithm can track permanently and efficiently the maximum power of the PV panel at any condition.

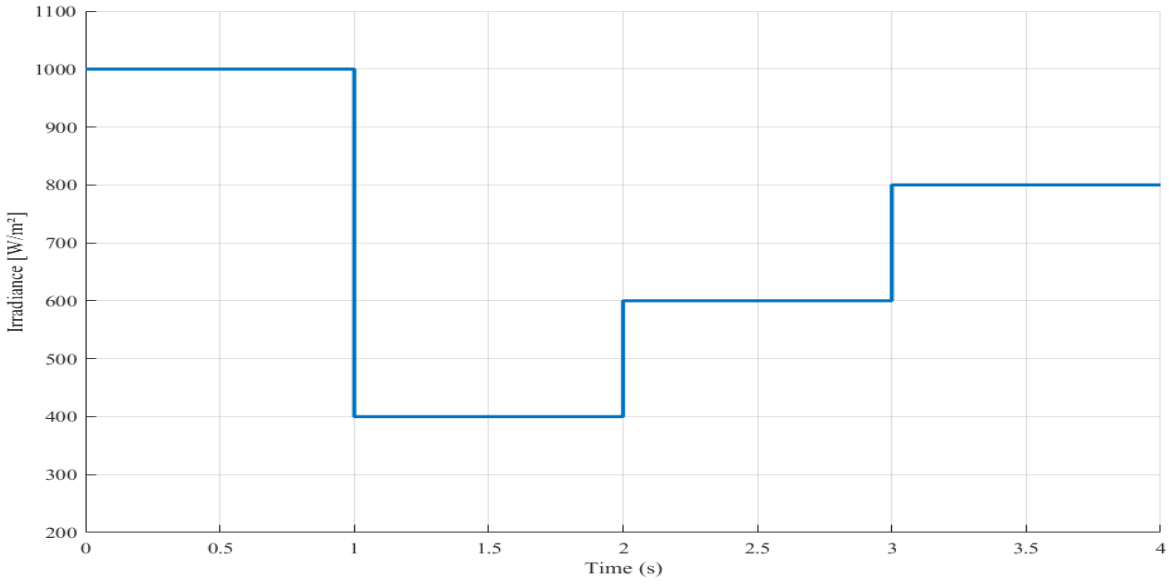

Figure II.20. The irradiance profile injected into the PV panel.

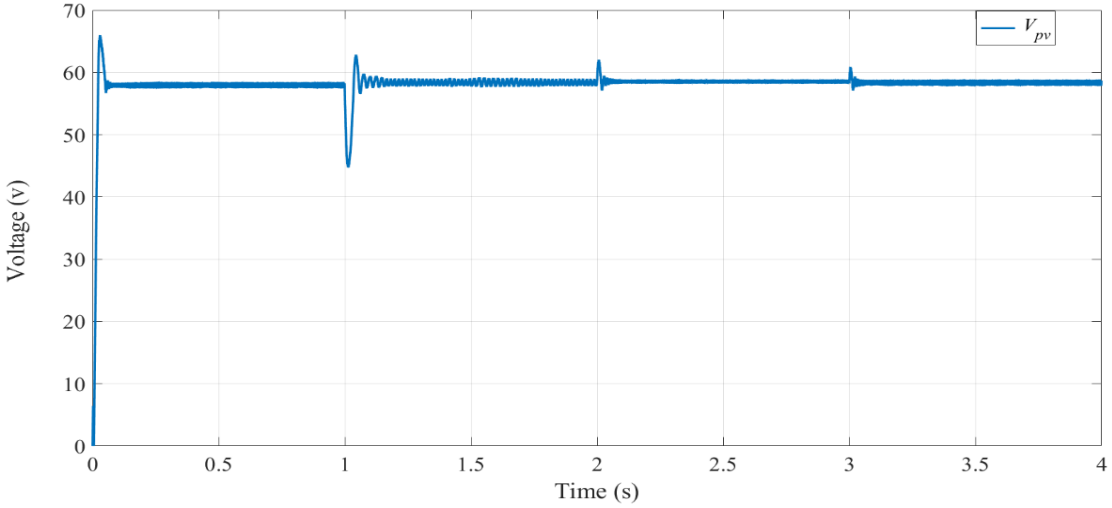

Figure II.21. PV voltage panel under sudden irradiance changes.

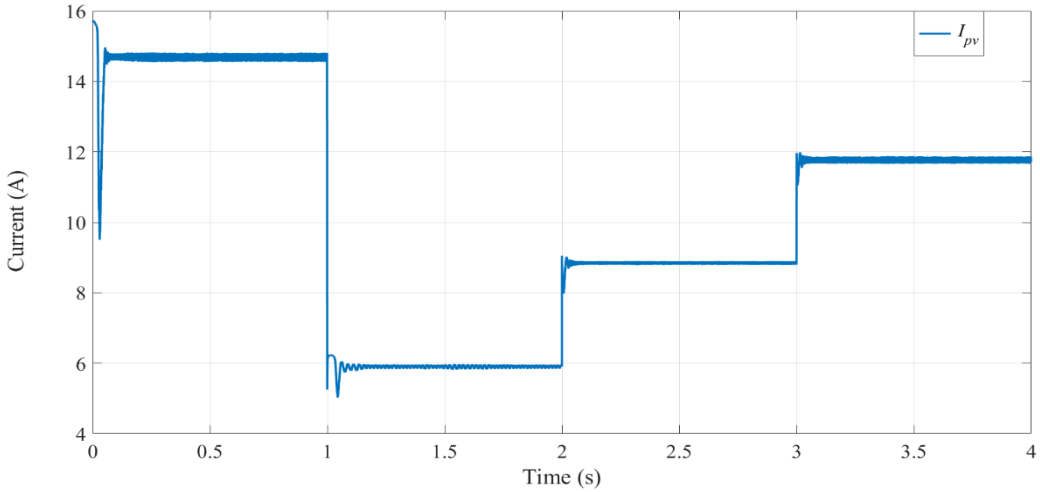

Figure II.22. PV current panel under sudden irradiance changes.

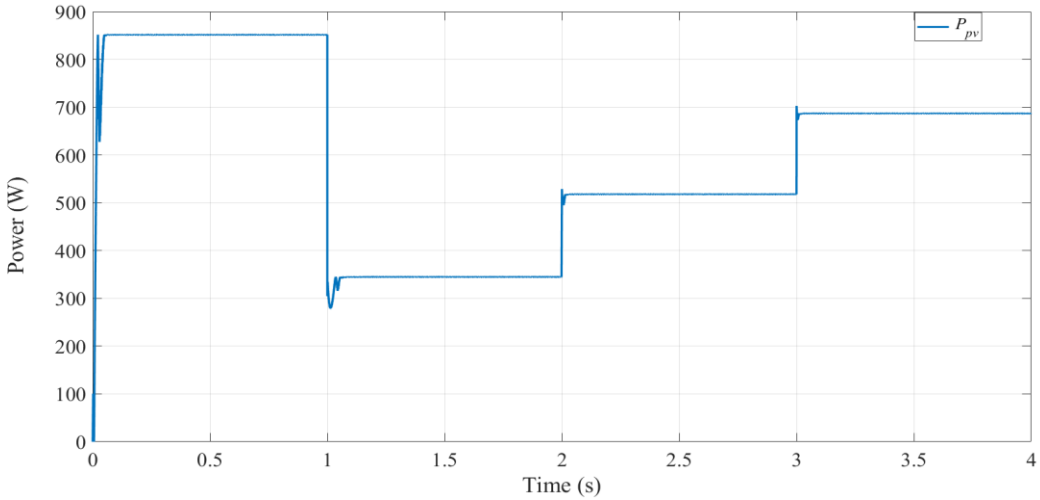

Figure II.23. PV power panel under sudden irradiance changes.

The simulated responses of the capacitors voltages are showed in Figure II.24. It can be observed that the capacitors voltages track their references with good accuracy and stability, regardless the irradiance variations.

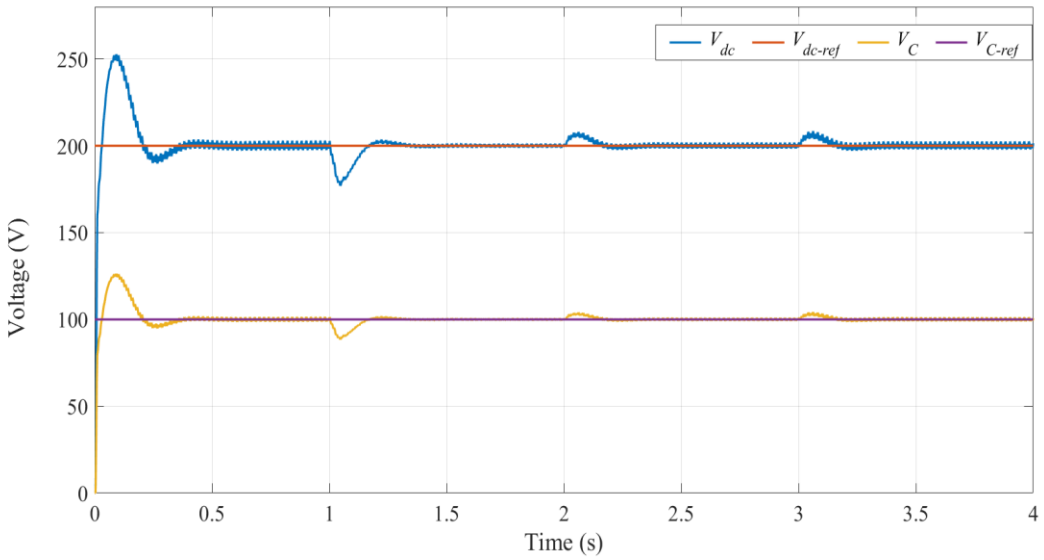

Figure II.24. Capacitors voltages waveforms under sudden irradiance changes.

The simulated responses of the grid voltage and current are plotted in Figure II.25. It can be noted that the grid current is in phase with the grid voltage, which proves the unity power factor operation.

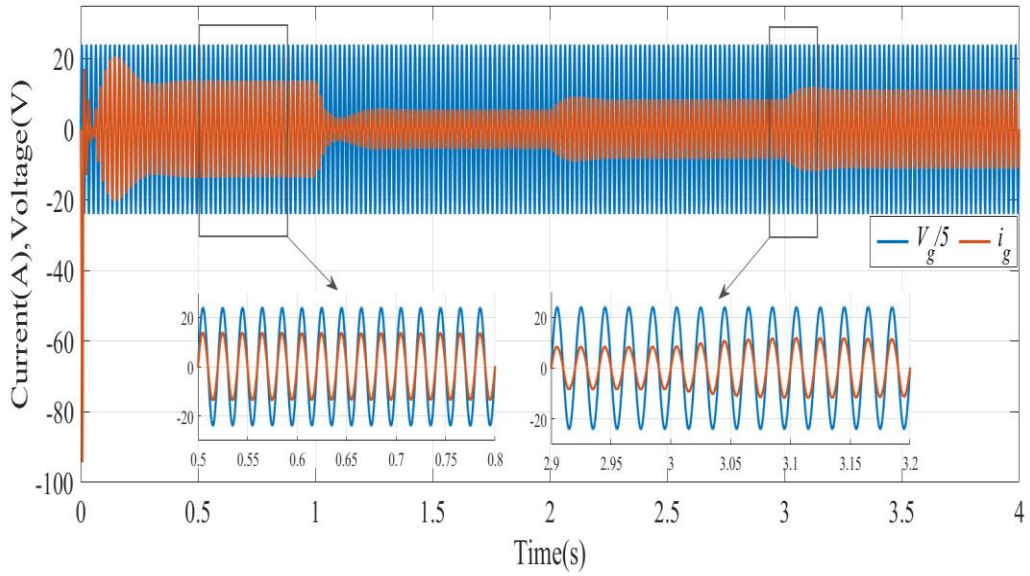

Figure II.25. Waveforms of grid voltage and current under sudden irradiance changes.

Figure II.26 shows the simulated response of the grid current tracking performance for the MPC algorithm. It can be seen that the MPC algorithm tracks excellently the reference of grid current under different levels of irradiance. The simulated response of PUC5 output voltage is presented in Figure II.27. It can be noted that PUC5 generates 5-level output voltage which proves the effectiveness of the suggested MPC algorithm.

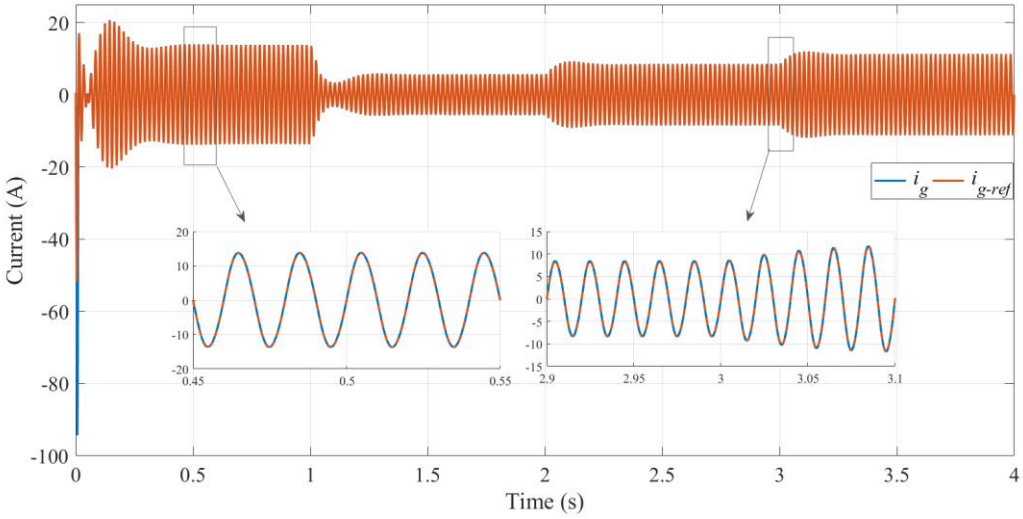

Figure II.26. Waveform of injected grid current under sudden irradiance changes.

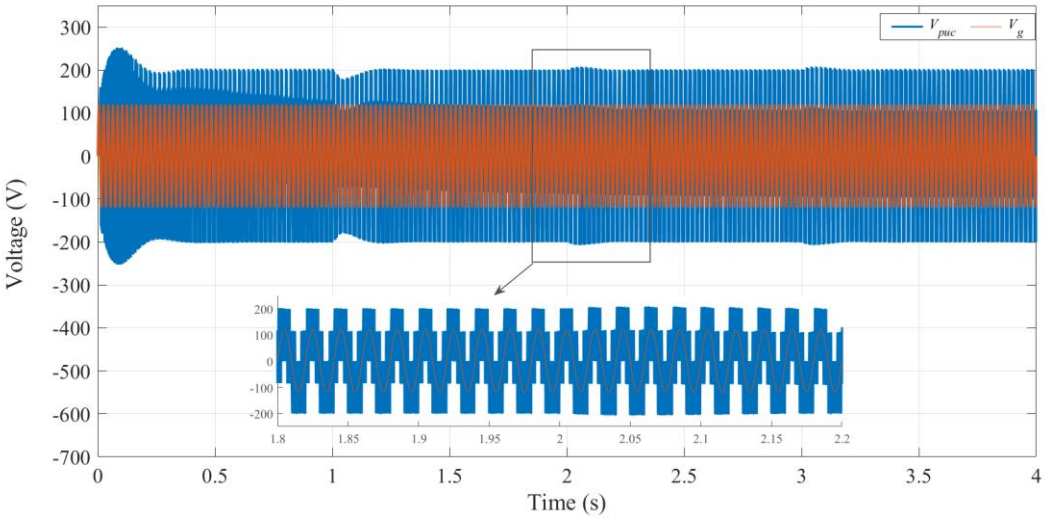

Figure II.27. Waveform of PUC5 output voltage under sudden irradiance changes.

In order to prove the performance of the suggested MPC algorithm, a comparative study with a conventional control scheme based on linear PI regulator in terms of the injected gird current quality (THDi %) is presented. Figure II.28 shows the classical PI controller approach for the PUC5 using MATLAB/Simulink.

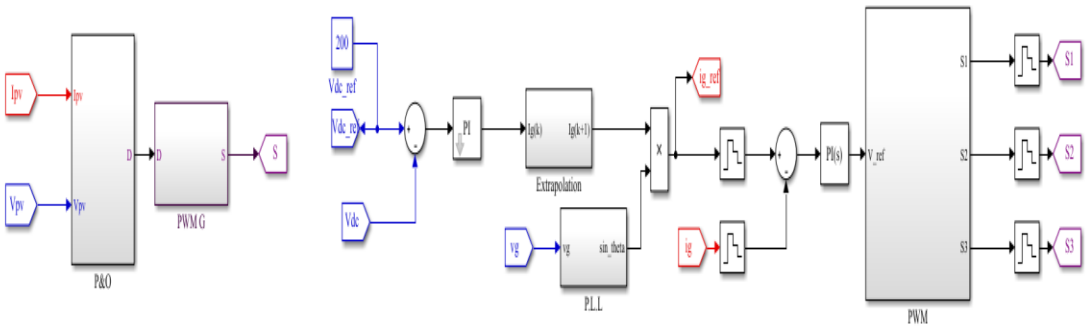

Figure II.28. Classical PI controller approach for the PUC5 under study.

Figures II.29 and 30 compare the performance of the suggested control system with classical PI control system under irradiance levels. It can be observed that the suggested control system offers good performance in terms of injected grid current quality (THDi %). Table II.4 summarize the comparison study.

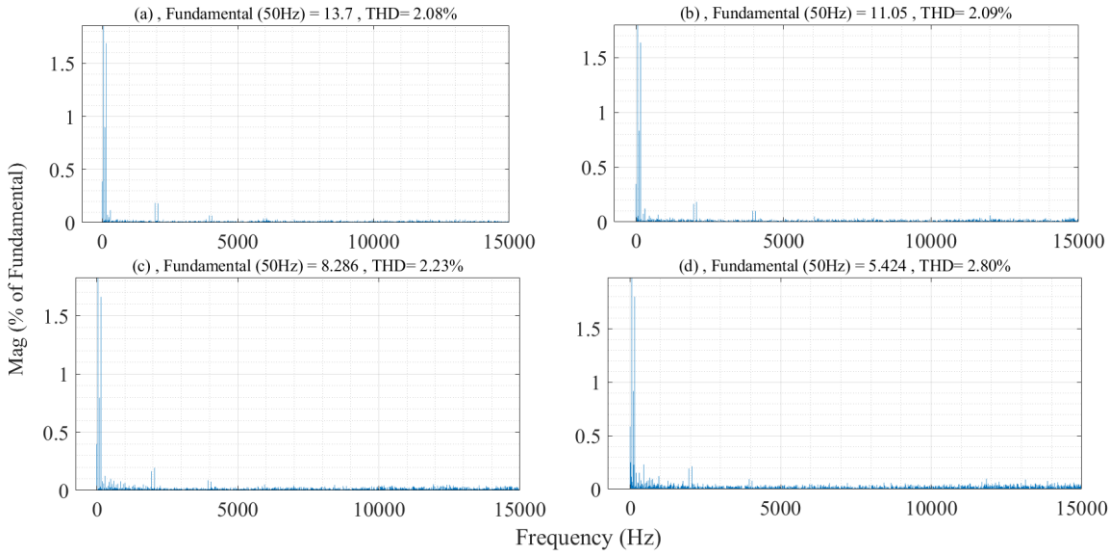

Figure II.29. FFT analysis of grid current with MPC algorithm in different irradiation ((a) ➔1000 W/m², (b) ➔800 W/m² , (c) ➔600 W/m² , (d) ➔400 W/m²)

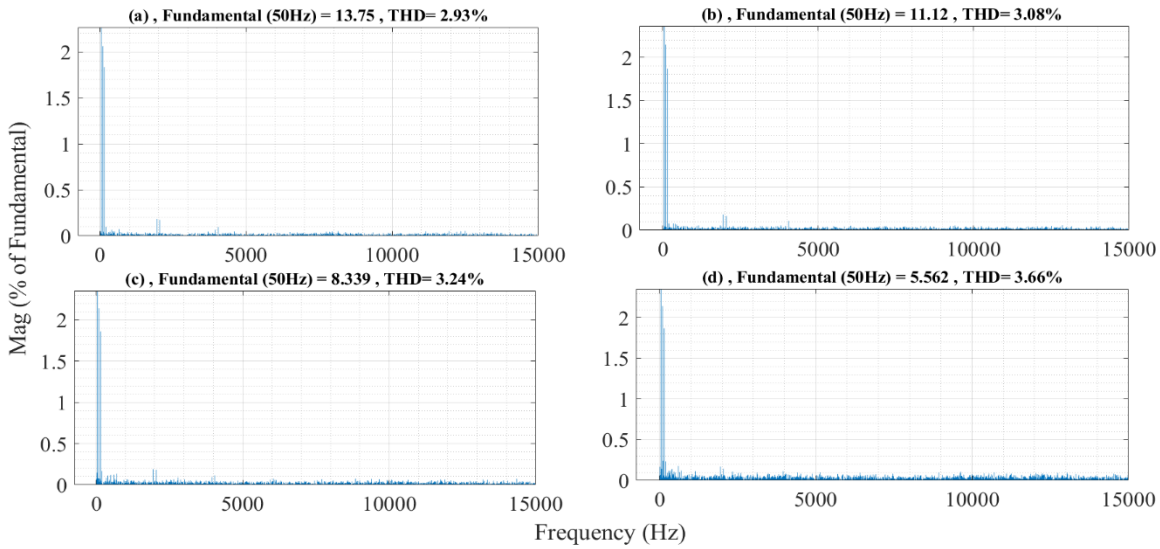

Figure II.30. FFT analysis of grid current with classical PI controller in different irradiation ((a) ➔1000 W/m², (b) ➔800 W/m² , (c) ➔600 W/m² , (d) ➔400 W/m²))

Table II.4. Comparison of grid current THD % under sudden irradiance changes.

Irradiance (w/m^2)	1000	800	600	400
Regulator PI	2.08	2.09	2.23	2.8
Suggested MPC	2.93	3.08	3.24	3.66

II.6. Conclusion

In this chapter, a control scheme based on model predictive control for single-phase grid-connected PV system using PUC5 inverter is suggested and discussed. The simulation results show a good tracking performance for the maximum power points of the PV array under sudden irradiance changes. Moreover, the studied grid-connected PV system with the suggested MPC algorithm injects the PV power with high grid current quality compared to the classical PI controller in different irradiance changes levels.

General conclusion

This work is a Master's thesis in Electronic Industries carried out at the University Of Mohamed El-Bachir El Ibrahimi on the optimization of the integration of the PV energy in the grid utility. The objective of this work is to design an effective control scheme for a single-phase PV system connected to the utility grid.

In this context, we have presented and modelled a single-phase grid-connected PV system, consisting of mainly of a PV array, DC-DC Boost converter and PUC5 inverter. PUC5 converter is a promising topology to interface the PV system to grid with less harmonic filters and high efficiency. It can provide 5-level output voltage with only single DC source and six power switches. A control scheme based on P&O MPPT algorithm and model predictive control (MPC) is suggested. The purposes of the suggested controller scheme are :

- Track the maximum power point rapidly and accurately under sudden irradiance changes using P&O algorithm.
- Generate a pure symmetrical synchronized 5 level voltage in PUC5 output.
- Ensure a high quality with a reasonable THD% value of the injected currents into the grid.

To show the performance improvement of the suggested control systems, a completed simulation models have developed using MATLAB/Simulink. The obtained results indicated the excellent performance of the proposed control schemes compared to the classical PI controller.

The following future research works are suggested as an extension to the knowledge presented in this thesis:

- Comparison of MPC controllers with other control techniques.
- Possibility to connect this topology to different other renewable energy sources.

REFERENCES

[1] Manisha Joshi. Prof.Dr. Mrs.G.A. Vaidya. Modeling and Simulation of Single-Phase Grid Connected Solar Photovoltaic System. Article. IEEE. INDICON. 2014. https://ieeexplore.ieee.org/document/7030623.

[2] Bader Nasser Alajm. Design and Control of Photovoltaic Systems in Distributed Generation. Doctoral thesis. University of Strathclyde. 2013. https://ethos.bl.uk/OrderDetails.do?uin=uk.bl.ethos.576436.

[3] By S. Ashok https://www.britannica.com/science/solar-energy

[4] G. Boyle. Renewable Energy: Power for a Sustainable Future, 2nd ed. Oxford, UK: Oxford University Press, 2004.

[5] Manisha Joshi. Prof.Dr. Mrs.G.A. Vaidya. Modeling and Simulation of Single-Phase Grid Connected Solar Photovoltaic System. Article. IEEE. INDICON. 2014.https://ieeexplore.ieee.org/document/7030623.

[6] Bader Nasser Alajm. Design and Control of Photovoltaic Systems in Distributed Generation. Doctoral thesis. University of Strathclyde. 2013. https://ethos.bl.uk/OrderDetails.do?uin=uk.bl.ethos.576436

[7] https://hardwarebee.com/what-is-dc-dc-converters/

[8] Vahedi, H. (2016). Modeling, development and control of multilevel converters for power system application (Doctoral dissertation). École de technologie supérieure, Canada.

[9] Faycel, Salah Eddine (2021). Study and control of qZ source inverter for grid-connected photovoltaic system. (MASTER)University of Mohamed El-Bachir El-Ibrahimi - Bordj Bou Arreridj-BBA.

[9] Hadji Slimane. Optimisation de la conversion énergétique pour les systèmes à énergie Photovoltaïque. 2018. Thèse de doctorat. Université Ferhat Abbas Sétif 1, Algérie.

[10] Behir Boubaker, Khemida Fathi et Guetroune Kheir eddine. Optimisation d'un système photovoltaïque adapté par une commande MPPT floue. 2019. Mémoire de master. Université Echahid Hamma Lakhdar El Oued, Algérie.

[11] Rekioua Djamila, Matagne Ernest. Optimization of photovoltaic power systems. 2012. Springer Verlag.

[12] SOUISSI & MESSAGIER (2020), Etude comparative des commandes MPPT conventionnelles et avancées pour les applications photovoltaïques, (Master) University BBA

[13] Vahedi, H., Kanaan, H. Y., & Al-Haddad, K. (2015), PUC Converter Review: Topology, Control and Applications, Ecole de Technologie Superieure, University of Quebec, Montreal,

[14] Sahli, A. (2021). Optimisation de la qualité d'énergie dans les Smart grids (Doctoral dissertation). University Ferhat Abbas – Sétif.

[15] Fadia assaad Sebaaly, Hani Vahedi, Hadi Kanaan, Kamal Al-Haddad, (2018), Experimental Design of Fixed Switching Frequency Model Predictive Control for Sensor-Less Five-Level Packed U-Cell Inverter, IEEE Transactions on Industrial Electronics.

[16] Vahedi, H., Labbé, P. A., & Al-Haddad, K. (2015). Sensor-less five-level packed U-cell (PUC5) inverter operating in stand-alone and grid-connected modes. IEEE Transactions on Industrial Informatics, 12(1), 361-370.

Abstract

This work describes a single-phase grid-connected photovoltaic (PV) system with five level PUC topology using the perturb and observe (P&O) MPPT (maximum power point tracking) algorithm and model predictive control (MPC) technique. The studied system consists of two stages: a PV panel with a DC-DC boost converter and PUC5 multilevel inverter with three pairs of switches. This topology have the ability to generate five voltage levels with a smaller number of active and passive components comparing with conventional multilevel inverter topologies. The suggested control technique aims to tracking the maximum power from PV panel and to reducing the total harmonic distortion (THD) of the grid injected current. The simulation results show a good tracking performance for the maximum power points of the PV array under sudden irradiance changes. Moreover, the studied grid-connected PV system with the suggested MPC algorithm injects the PV power with high grid current quality compare to the classical PI controller in different irradiance changes levels.

Keywords: *single-phase grid-connected photovoltaic system, model predictive control, perturb and observe MPPT algorithm.*

Résumé

Ce travail décrit un système photovoltaïque (PV) monophasé connecté au réseau avec une topologie PUC à cinq niveaux utilisant l'algorithme de perturbation et observation (P&O) MPPT (maximum power point tracking) et la technique de contrôle prédictif (MPC). Le système étudié se compose de deux étages : un panneau PV avec un convertisseur boost DC-DC et un onduleur multiniveaux PUC5 avec trois paires de commutateurs. Cette topologie à la capacité de générer cinq niveaux de tension avec un plus petit nombre de composants actifs et passifs par rapport aux topologies conventionnelles d'onduleurs multi- niveaux. La technique de contrôle suggérée vise à suivre la puissance maximale du panneau PV et à réduire la distorsion harmonique totale (THD) du courant injecté dans le réseau. Les résultats de simulation montrent une bonne performance de suivi pour les points de puissance maximum du générateur photovoltaïque sous des changements soudains d'irradiance. De plus, le système PV connecté au réseau étudié avec l'algorithme MPC suggéré injecte la puissance PV avec une qualité de courant de réseau élevée par rapport au contrôleur PI classique dans différents niveaux de changements d'irradiance.

Mots-clés : système photovoltaïque monophasé connecté au réseau, contrôle prédictif, algorithme de perturbation et observation MPPT.

ملخص

يصف هذا العمل نظامًا ضوئيًا أحادي الطور متصل بالشبكة (PV) مع خمسة طوبولوجيا PUC باستخدام خوارزمية الاضطراب والمراقبة MPPT (P&O) (تتبع نقطة الطاقة القصوى) وتقنية التحكم التنبئي النموذجي .(MPC) يتكون النظام المدروس من مرحلتين: لوحة PV مع محول تعزيز DC-DC وعاكس متعدد المستويات PUC5 مع ثلاثة أزواج من المفاتيح. تتمتع هذه الهياكل بالقدرة على توليد خمسة مستويات من الجهد مع عدد أقل من المكونات النشطة والسلبية مقارنة بطوبولوجيا العاكس التقليدية متعددة المستويات. تهدف تقنية التحكم المقترحة إلى تتبع الطاقة القصوى من اللوحة الكهروضوئية وتقليل التشوه التوافقي الكلي (THD) للتيار المحقون بالشبكة. تُظهر نتائج المحاكاة أداء تتبع جيدًا لأقصى نقاط طاقة لمجموعة PV تحت تغييرات الإشعاع المفاجئة. علاوة على ذلك ، فإن النظام الكهروضوئي المتصل بالشبكة المدروس مع خوارزمية MPC المقترحة يضخ الطاقة الكهروضوئية بجودة تيار شبكي عالية مقارنة بوحدة تحكم PI الكلاسيكية في مستويات مختلفة من تغيرات الإشعاع.

الكلمات الرئيسية: النظام الكهروضوئي أحادي الطور المتصل بالشبكة ، والتحكم التنبئي النموذجي ، والاضطراب ومراقبة خوارزمية MPPT.